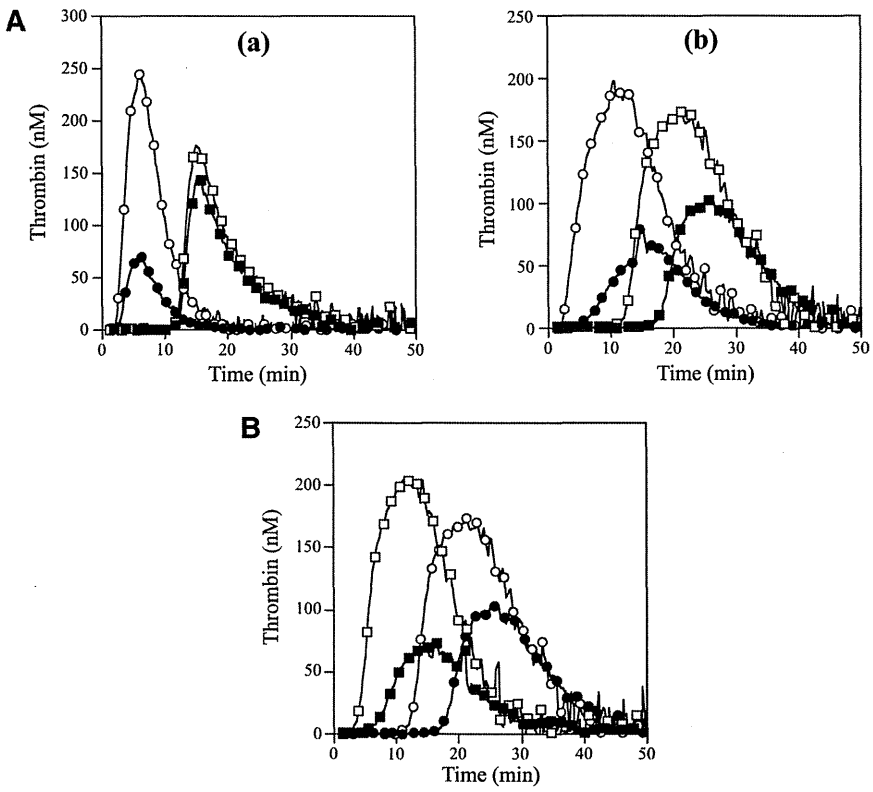

Figure 2. Thrombin generation in the FV_{Nara} patient's plasma. (A) Effects of the addition of APC: thrombin generation after extrinsic activation (TF; 5 pM) of PPP (a) or PRP (b) in normal individuals (circle symbols) and PPP (a) or PRP (b) in FV_{Nara} patient (square symbols) in the absence (open symbols) or presence (closed symbols) of APC was measured as described in "Materials and methods." With PPP, APC (8 nM) was added with PL vesicles (10 μM), whereas with PRP, APC (40 nM) was added without PL. A representative thrombogram is shown. (B) Effects of the addition of native FV: thrombin generation was measured after extrinsic activation (TF; 5 pM) of the patient's PRP with the addition of native FV (circles, 0 IU/dL; squares, 10 IU/dL) in the absence (open symbols) or presence (closed symbols) of APC (40 nM). All experiments were performed at least 3 separate times, and a representative thrombogram is shown.

APCR in the FV_{Nara} patient was examined using PPP in thrombin generation assay initiated by low concentrations of TF with APC. The time-related parameters (lag time and time to peak) and peak thrombin obtained with FV_{Nara} PPP were prolonged and decreased, respectively, compared with control (Figure 2Aa and Table 2). The addition of APC showed that the peak thrombin and ETP with FV_{Nara} were less moderated than those with control, although the time-related readings were unaffected. The APCsrs (minus APC/plus APC) with FV_{Nara} (1.22 and 1.25) were significantly lower than those with control (3.48 and 3.70), supportive of the APCR with FV_{Nara}. Platelet FV also participates in the clotting function of FV; to evaluate the role of platelet FV in these mechanisms, therefore, experiments were repeated using PRP. Similar to PPP, the addition of APC showed that APCsrs (plus APC/minus APC) in time-related parameters in FV_{Nara} were lower than those in control, and the APCsrs (minus APC/plus APC) with FV_{Nara} were also lower than those with control (Figure 2Ab). These findings provided further evidence of APCR with FV_{Nara}. Similar experiments in PPP using 40 nM APC (equal amount in PRP) showed that the thrombin generation of FV_{Nara}, as well as normal plasma, was little detected (data not shown), again confirming that the platelet FV was particularly resistant to APC-mediated inactivation.

To further assess the contribution of plasma FV in the APCR of FV_{Nara}, normal FV was added to the patient's PRP before measuring thrombin generation with APC (Figure 2B). In the presence of normal FV (10 IU/dL) corresponding to the level in patient's plasma, the time-related parameters were moderately shortened, and the peak thrombin and ETP were slightly increased. Thus, the presence of native FV improved reactivity to APC in FV_{Nara} PRP, suggesting that the APCR of FV_{Nara} might be caused by defective patient's plasma FV. Furthermore, even small amounts of plasma FV appeared to influence APC-induced deceleration of blood coagulation.

APC cofactor activity of FV_{Nara}

APCR resulting from a *F5* mutation or mutations is caused by a reduced sensitivity of FVa to APC-catalyzed inactivation[7,32] and/or reduced FV cofactor activity in APC-catalyzed FVIIIa inactivation,[33] but these components are difficult to distinguish. FXa generation

Table 2. Parameters obtained from thrombin generation on the PPP and PRP with FV_{Nara}

	Lag time (APC minus/plus, minutes [APCsr])*	Time to peak (APC minus/plus, minutes [APCsr])*	Peak thrombin (APC minus/plus, nM [APCsr])†	ETP (APC minus/plus, nM × minutes [APCsr])†
PPP				
Control	2.50/2.62 (1.05)	6.12/5.62 (0.92)	242/70 (3.48)	1648/446 (3.70)
FV_{Nara}	12.3/12.5 (1.02)	15.3/15.3 (1.00)	176/144 (1.22)	1711/1373 (1.25)
PRP				
Control	3.01/6.55 (2.18)	11.5/15.7 (1.36)	191/71 (2.69)	2860/968 (2.95)
FV_{Nara}	12.8/18.2 (1.42)	21.2/26.2 (1.23)	169/103 (1.64)	2811/1620 (1.74)
+ FV (10 IU/dL)	2.86/6.45 (2.25)	11.5/16.2 (1.42)	201/70 (2.87)	2988/930 (3.21)

Values were calculated from the parameter data obtained in Figure 2.
*Values were expressed as plus APC divided by minus APC.
†Values were expressed as minus APC divided by plus APC.

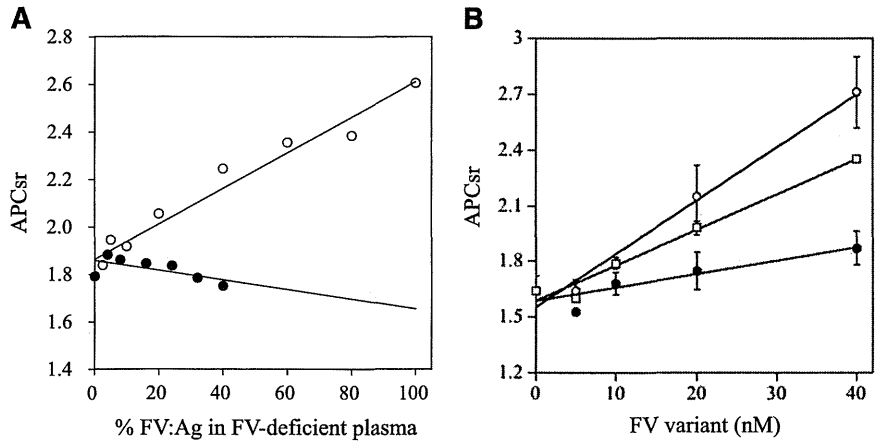

Figure 3. APCR in FXa generation assays. (A) Effects of FV levels on the APCsr in the FV_{Nara} plasma. Normal plasma (open circles) and the patient's plasma (closed circles) were mixed with FV-deficient plasma in various proportions, and FXa generation was measured with COATEST SP FVIII after the simultaneous addition of APC (40 nM) as described in "Materials and methods." The APCsrs were expressed as ratios of the amount of generated FXa in the absence of APC divided by that in its presence. All experiments were performed at least 3 separate times, and the average values are shown. (B) APCR of FV-deficient plasma mixed with recombinant FV-W1920R. Various concentrations of FV (WT, open circles; W1920R, closed circles; R506Q, open squares) were mixed with diluted FV-deficient plasma, and FXa generation was measured with COATEST SP FVIII after the simultaneous addition of APC (40 nM), as described in "Materials and methods." The APCsrs were expressed as ratios of the amount of generated FXa in the absence of APC divided by that in its presence. All experiments were performed at least 3 separate times, and the average and/or standard deviation values are shown.

assays, reflecting intrinsic tenase activity, were used to examine the APC cofactor activity of FV.[27] We therefore determined APCsrs in samples after the addition of APC to probe APCR resulting from defective FV cofactor activity. Normal or FV_{Nara} plasma was mixed with FV-deficient plasma in proportions from 2.5% to 100%. Because FV_{Nara}:Ag was 40 IU/dL, the concentration of FV_{Nara} in these assays varied between 2.5% and 40%. APCsrs increased linearly in proportion to the level of normal FV, and clear differences were demonstrated between 0% and 100% normal plasma (1.8 and 2.6, respectively), similar to an earlier report.[27] APCsrs were independent of the concentration of FV_{Nara}, however, and remained relatively constant or modestly decreased (Figure 3A). The slopes obtained with normal and FV_{Nara} plasmas (ΔAPCsr; 0.72 and −0.18/IU FV, respectively) were significantly different ($P < .01$), indicating that FV_{Nara} possessed little APC cofactor activity.

APCR of FV-W1920R mutant

The measurements of APCR of FV_{Nara} could have been affected by quantitative or qualitative abnormalities of individual plasma components other than FV. To confirm FV specificity, recombinant FV-WT and 2 FV mutant proteins (W1920R and R506Q) were prepared. The levels of FV:Ag and specific activity of the W1920R mutant expressed in CM were similar to the data observed with patient's plasma, at 50% and 45% of WT, respectively. Corresponding levels in CM of R506Q were 125% and 86% of WT, respectively.

APCR assays were repeated using mixtures of FV-deficient plasmas and recombinant FV variants. FXa generation assays were devised in which FV-deficient plasma and FV were diluted 16-fold before mixing with APC; this facilitated measurements at lower levels of FV:Ag (0.3-2.5 nM). These concentrations were comparable to diluted plasma containing physiological levels of FV:Ag (5-40 nM;

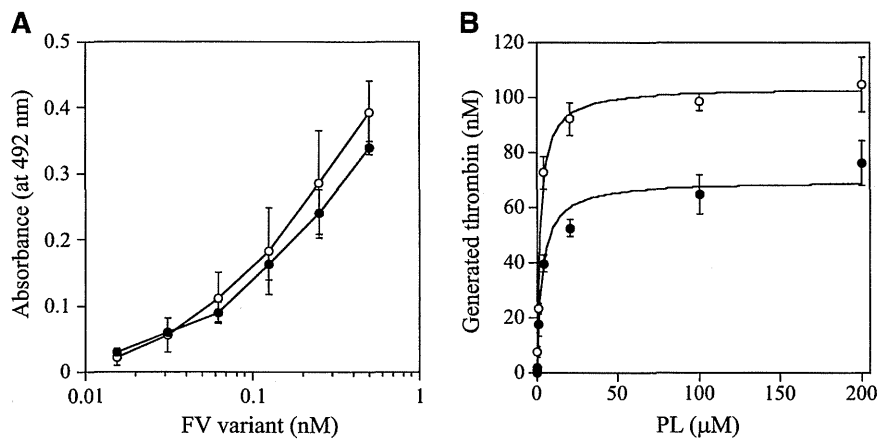

Figure 4. FV-W1920R affecting the association with PL. (A) FV-PL binding. α-Phosphatidyl-L-serine (5 μg/mL) was added to microtiter wells and air-dried. After blocking, serial dilutions of FV were added to the immobilized PL. Bound FV-WT (open circles) and FV-W1920R (closed circles) was quantified by the addition of AHV-5146, as described in "Materials and methods." The average values and standard deviations are shown. (B) The effects of PL on prothrombinase activity; FV (WT, open circles; W1920R, closed circles; 2 nM) was activated by thrombin (20 nM) for 1 minute, followed by the addition of hirudin. The reactants were incubated with prothrombin (1.4 μM) and various amounts of PL, followed by initiation by the addition of FXa (10 pM). Aliquots were removed, and the reactions were quenched by the addition of EDTA. Rates of thrombin generation were determined at Abs_{405} after the addition of S-2238. Thrombin generation was quantified by extrapolation from a standard curve prepared using known amounts of thrombin. The plotted data were fitted using the Michaelis-Menten equation. All experiments were performed at least 3 separate times, and the average values are shown.

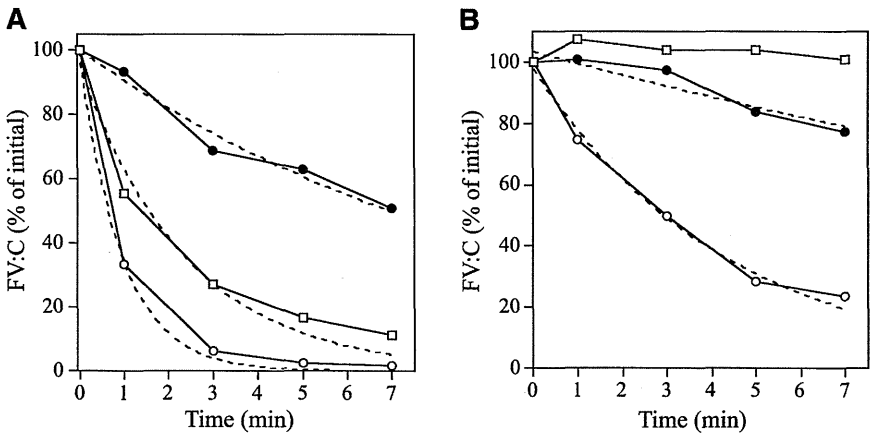

Figure 5. APC-mediated inactivation of FVa-W1920R mutant. FV variants (8 nM) were incubated with thrombin (100 nM) for 5 minutes, and the reaction was terminated by the addition of hirudin (25 U/mL). FVa variant samples (2 nM) were reacted with APC (25 pM) and PL (20 μM) in the presence (A) or absence (B) of PS (30 nM). After dilution, FVa activity was measured in an aPTT-based 1-stage clotting assay. The symbols used are as follows: open circles, WT; closed circles, W1920R; open squares, R506Q. Initial activities of FVa variants were regarded as 100%. The plotted data were fitted in an equation of single exponential decay. All experiments were performed at least 3 separate times, and the average values are shown.

15%-120% of normal FV:Ag). In mixtures with WT, APCsrs increased dose-dependently (ΔAPCsr; 2.85 × 10^{-2}/nM FV; Figure 3B). The APCsr in W1920R was lower by ~4-fold (0.71 × 10^{-2}/nM FV) than WT, in keeping with the impairment of APC cofactor activity in W1920R. With R506Q, the APCsr was greater by ~2.7-fold (1.91 × 10^{-2}/nM FV) than that with W1920R. These findings demonstrated that APCR in FV_{Nara} plasma resulted from W1920R, and the APC cofactor activity of W1920R appeared to be more defective than that of R506Q.

The C1 and/or C2 domains of FV(a) bind to PL membranes,[34,35] which governs the susceptibility of FVa for APC-catalyzed inactivation and the APC cofactor activity of FV. W1920 is in proximity to the PL-binding region or regions,[36] and we speculated that the APCR of FV-W1920R might be a result of significant disturbances in PL binding. The PL binding of W1920R was maintained at ~90% that of WT in ELISA, however (Figure 4A). The influence of PL on prothrombinase activity with W1920R was also investigated. Thrombin generation with W1920R was ~70% the level of that with WT, again supporting the cross-reactive material–reduced type on FV_{Nara}. However, the affinity of PL for W1920R was not significantly different compared with WT (K_m: 3.25 ± 0.77/2.22 ± 0.24 μM, respectively; Figure 4B). Thrombin and PL-dependent FXa activation of W1920R showed a similar reaction to the activation of WT (data not shown). These findings indicated that W1920R–PL interactions were not disturbed.

APC-catalyzed inactivation of FVa-W1920R

APC-catalyzed inactivation of FVa-W1920R, compared with the inactivation of WT and R506Q (FV_{Leiden}), were examined in 1-stage clotting assays. FVa-WT:C was very rapidly decreased after the addition of APC and PS and declined to ~2% of the initial level at 5 minutes (Figure 5A). FVa-R506Q:C was reduced to ~20% of the initial level at 5 minutes. Surprisingly, FVa-W1920R:C decreased very slowly and persisted at ~60% of the initial level. The inactivation rate of W1920R was ~11- and ~4.5-fold lower than the rates of WT and R506Q, respectively (Table 3), indicating significantly defective APC-induced inactivation of W1920R. Without PS, the inactivation rate of FVa-WT:C was significantly decreased, with ~20% of the rate obtained with PS (Figure 5B), whereas inactivation of FVa-R506Q:C was not observed. The inactivation rate of FVa-W1920R:C appeared to be ~40% less than that with PS, but this was ~6-fold lower than that of WT, supporting the theory that W1920R as a cofactor for PS contributed less to the mechanisms of APCR than WT and R506Q.

Sodium dodecyl sulfate/polyacrylamide gel electrophoresis of APC cleavage was designed to investigate the mechanism or mechanisms contributing to the defective APC-catalyzed inactivation of FVa-W1920R (Figure 6). Using FVa-WT, the band of residues 1 to 506 rapidly appeared within 20 seconds after the addition of APC, followed sequentially by the appearances of the 307 to 506 and 307 to 709 bands, consistent with rapid, consecutive cleavage at Arg506 and Arg306. Cleavage of FVa-R506Q at Gln506 was not evident during a 5-minute reaction. The appearance of the 307 to 709 band was evident at similar velocity to that in WT, but the total ratio of Arg306 cleavage in R506Q was reduced. The appearance of the 1 to 506 band in W1920R was markedly delayed compared with WT, however, and cleavage at Arg306 was not detected. These results suggested that the loss of APC-catalyzed inactivation of FVa-W1920R was a result of a significant delay in cleavage at Arg506 and little cleavage at Arg306.

Cofactor FV-W1920R on APC-catalyzed FVIIIa inactivation

Properties of FV-W1920R as a cofactor for APC were examined in a FVIIIa degradation assay.[29] FV-WT significantly enhanced APC-catalyzed FVIIIa inactivation with a ~3-fold inactivation rate compared with that in its absence, again confirming the APC cofactor activity of FV (Figure 7Aa and Table 4). FV-R506Q moderately diminished APC-catalyzed inactivation with the ~50% inactivation rate of WT. However, the rate with W1920R was similar to that in its absence, emphasizing earlier findings that APC cofactor activity was markedly depleted with W1920R. With regard to the effects of varying amounts of FV on APC cofactor activity, FV-WT enhanced the APC-catalyzed inactivation dose-dependently (50% reduction, 0.25 nM) (Figure 7Ab). Inactivation with R506Q was also enhanced, but the 50% reduction of 0.55 nM was greater than that with WT. However, even at 1 nM of W1920R, little enhancement of this mechanism was demonstrated, indicating that impairment of APC cofactor activity with W1920R was more pronounced than with R506Q.

Table 3. Kinetic parameters determined on APC-catalyzed inactivation of recombinant FVa variants

FVa variants	PS, minutes^{-1} (-fold)	
	Plus	Minus
WT	1.07 ± 0.06 (1)	0.230 ± 0.016 (1)
W1920R	0.100 ± 0.001 (0.09)	0.038 ± 0.008 (0.16)
R506Q	0.417 ± 0.061 (0.39)	Not determined

Values were calculated by nonlinear least squares regression from the data shown in Figure 5A-B, using the single exponential decay.

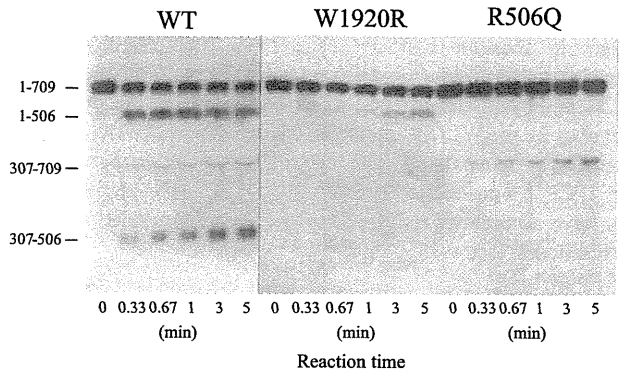

Figure 6. APC-catalyzed proteolytic cleavage of the HCh of FVa-W1920R. FV variants (8 nM) were incubated with thrombin (100 nM) for 5 minutes, and the reaction was terminated by the addition of hirudin (25 U/mL). FVa variant samples (0.5 nM) were incubated with APC (1 nM) and PS (30 nM) in the presence of PL (20 μM) for the indicated times. Samples were analyzed on 8% gels, followed by western blotting using an anti-FV HCh mAb 5146 IgG, as described in "Materials and methods." A vertical line is inserted to indicate a repositioned gel lane.

APC-catalyzed FVIIIa inactivation is regulated by cleavage at Arg336 in A1.[37] Figure 7B illustrates time-dependent cleavage at Arg336 analyzed by western blotting using mAbC5. This mAb recognizes the residues 337 to 372, and the disappearance of this band represents cleavage at Arg336.[38] With FV-WT, intact A1 gradually decreased time-dependently (Figure 7Ba). With FV-W1920R, however, cleavage at Arg336 was not observed during a 10-minute reaction time, and the rate of cleavage with FV-R506Q appeared to be ~40% of that of FV-WT (Figure 7Bb and Table 4), consistent with the results obtained in FXa generation assays. These data confirmed that APC cofactor activity was partially or completely impaired with R506Q and W1920R, respectively.

Discussion

We described a novel FV-W1920R missense mutation associated with APCR in a Japanese boy with serious DVT. The APCR of FV_{Nara} was greater than that of FV_{Leiden} and involved a novel mechanism related to a significant inhibition of cleavage at both sites because of the possible failure of direct and/or indirect interactions with APC and/or PS.

FV-W1920 is a highly conserved residue among other mammalians. According to the crystal structure of APC-inactivated bovine FVa,[36] bovine-W1907 (corresponding to human-W1920) is located on the internal structure in the C1 domain, which is involved in 3 spike-like structures of β-strand as PL-binding sites. W1907 forms hydrogen bonding with W1891 (W1904) and L2013 (L2026), which is located at the first and second spike of PL-binding, respectively. W1920R may have an effect on the PL binding at the C1 interface and may be an unstable molecule by modification (eg, misfolding). However, because a functional assay such as prothrombinase activity, FXa activation, and a PL-binding assay did not indicate significant differences between WT and W1920R, this molecule would be not significantly disturbed structurally; thereby, the reason for secretion defect is unclear.

Our assays for APC-catalyzed FV cleavage demonstrated little cleavage of W1920R at Arg306, and cleavage at Arg506 was markedly delayed. As discussed earlier, the Arg506 cleavage is considered to be essential for direct and FVIII-related anticoagulant properties of FV,[15,16,29] whereas the Arg306 cleavage is associated with FVa inactivation. Mutations at Arg306, including $FV_{Cambridge}$, contribute to mild APCR, and a similar mutation $FV_{Hong\ Kong}$, appears not to affect the APC response.[19-21] We speculate, therefore, that the impairment of APC-catalyzed cleavage at Arg506 in FV_{Nara} resulted in persistent levels of FVIIIa:C and FVa:C and was the

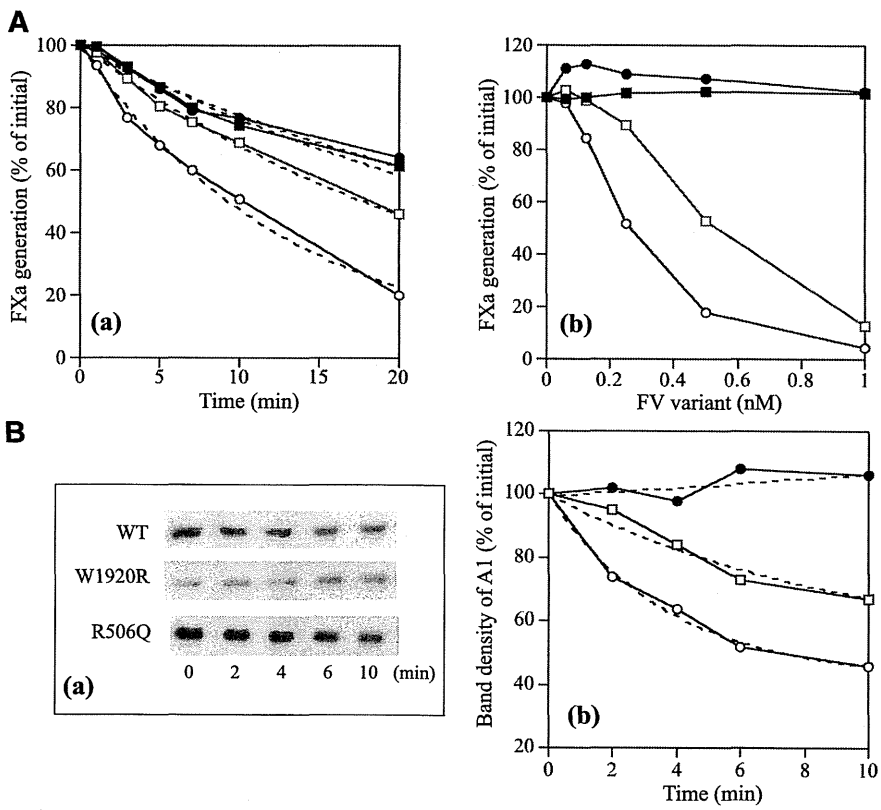

Figure 7. APC cofactor activity of FV-W1920R assessed by the degradation of FVIIIa. (A) FVIIIa inactivation. FVIII (10 nM) with PL (20 μM) was activated by thrombin (5 nM), followed by the addition of hirudin (2.5 U/mL). Generated FVIIIa was incubated either with mixtures of APC (0.5 nM), PS (5 nM), and FV variants (0.5 nM) for the indicated times (a) or with various concentrations of FV variants for 20 minutes (b). FXa generation was initiated by the addition of FIXa (2 nM) and FX (200 nM) for 1 minute. The symbols used are as follows: open circles, WT; closed circles, W1920R; open squares, R506Q; closed squares, no FV. Values of FXa generation at the initial time (a) or in the absence of FV variants (b) were regarded as 100%. The data in (a) were fitted on an equation of single exponential decay (dashed lines). All experiments were performed at least 3 separate times, and the average values are shown. (B) A1 cleavage at Arg336; FVIII (10 nM) with PL (20 μM) was activated by thrombin (5 nM) for 30 second, followed by the addition of hirudin (2.5 U/mL). Generated FVIIIa was incubated with mixtures of APC (0.5 nM), PS (5 nM), and FV variants (0.5 nM) for the indicated times. Samples were analyzed on 8% gels, followed by western blotting using an anti-A1 C5 IgG, as described in "Materials and methods" (a). Band densities of intact $A1^{1-372}$ observed from panel a were measured by quantitative densitometry. Density before the addition of APC was regarded as 100% (b). The plotted data were fitted in an equation of single exponential decay (dashed lines). The symbols used are as follows: open circles, WT; closed circles, W1920R; open squares, R506Q. All experiments were performed at least 3 separate times, and the average values are shown.

Table 4. Kinetic parameters determined on FVIIIa inactivation by APC and PS in the presence of recombinant FV variants

FV variants	Rate constant: k, $minutes^{-1}$ (-fold)	
	FVIIIa inactivation	Cleavage at Arg336
WT	0.742 ± 0.034 (1)	0.274 ± 0.034 (1)
W1920R	0.239 ± 0.021 (0.32)	Not determined
R506Q	0.390 ± 0.012 (0.53)	0.110 ± 0.076 (0.40)
None	0.246 ± 0.019 (0.33)	Not determined

Values were calculated by nonlinear least squares regression from the data shown in Figure 7A-B, using the single exponential decay.

most influential defect in the APCR mechanism. The complete loss of cleavage at Arg306 in FV_{Nara} also contributed to the stability of FVa:C. These findings provide potential new insights into the physiological role or roles of FV in (anti)coagulation systems.

The recurrence of DVT in FV_{Nara} was evident despite low levels of plasma FV:C. This observation appears to be unique in FV mutations reported with APCR. The precise reason or reasons for thrombotic symptoms in these circumstances remain to be clarified but could be explained by some laboratory features. First, moderately low levels of plasma FV:C (>5%) promote thrombin generation near to normal plasma and could facilitate significant effects on APCR. The thrombin-related procoagulant capacity of lower levels of FV:C (<2~3%) is very restricted, however, and the anticoagulant function of FV might be negligible. Second, platelet FV:C might be more important than plasma FV:C in physiological procoagulant activity.[39] Platelet FV:C in FV_{Nara} was ~20% (data not shown), and the peak level of thrombin formation in PRP was comparable to that of normal PRP (~90% of normal). The peak thrombin after the addition of APC was increased (145% of normal) (Figure 2Ab). Third, other hemostasis-related mechanisms may have a potential effect on the thrombotic diathesis. Other laboratory findings were within normal range in our patient, however, and we demonstrated directly that FV-W1920R conferred APCR.

The APCR mechanisms in FV_{Nara} appeared to be distinct from other APCR-associated FV mutations. With the exception of $FV_{Liverpool}$ (I359T),[40] all FV mutations have been identified in the HCh and constitute point mutations at cleavage sites that lead to the impairment of FV(a) inactivation. Delayed cleavage at Arg306 was described in $FV_{Liverpool}$, resulting in impaired inactivation of FVa and in clinically severe DVT. This mutation led to the creation of a glycosylation consensus sequence at Asn357 that is slightly remote from the Arg306 site. Cleavage at Arg506 in FVa and APC cofactor activity for FVIIIa inactivation was normal. However, W1920R is significantly remote from the APC-cleavage sites and from moderated cleavage at both Arg306 and Arg506. Although W1920 in FV is close to the PL-binding site,[36] the binding ability of W1920R to PL was almost equivalent to that of FV-WT, indicating that W1920R in FV_{Nara} might affect the direct association (binding-site) or indirect association (conformational change) with APC. In addition, W1920R was little cleaved by APC at Arg306, depending on PS, which might supporting a defective interaction with PS. Our conclusion that FV_{Nara} was resistant to APC inactivation through an impaired interaction with this protease might be further supported by observations that FVa-W1920R, when assembled into prothrombinase, was protected from FXa-catalyzed APC inactivation and that the inhibitory effect of FXa on APC-catalyzed inactivation of FVa-W1920R was observed, similar to WT (data not shown).

FV_{Leiden} is known to be a major cause of hereditary thrombotic diseases among Caucasians.[2,41] Studies of the ethnic distribution of FV_{Leiden} indicated that the mutation was not found in Asians.[17,18] A different FV mutation (E666D) causing APCR coupled with DVT has been reported in China,[42] but there are no reports of FV-associated APCR in Japan. The parents of the current propositus were heterozygous for the W1920R mutation, but they have not developed any thrombotic symptoms to date, although aPTT-based assays demonstrated mild APCR. It is possible that similar to FV_{Leiden}, the heterozygote FV_{Nara} may have a potential risk for thrombosis compounded by other prothrombotic factors.

Acknowledgments

We thank Dr Koji Yada, Dr Hiroaki Minami, and Dr Shoko Furukawa for the clinical support.

This work was partly supported by grants from Ministry of Education, Culture, Sports, Science and Technology (MEXT) Grants-in-Aid for Scientific Research (KAKENHI) (21591370 and 24591558 to K.N.) and an unrestricted research grant from Baxter (to K.F.).

Authorship

Contribution: K.N. and K.A. designed of research; K.N. and K.S. wrote the manuscript; K.N., K.S., K.O., and T.M. performed experiments; K.N., K.S., and K.O. analyzed the data; and K.F. and M.S. supervised the study, interpreted data, and edited the manuscript.

Conflict-of-interest disclosure: K.S. is an endowed assistant professor funded by Baxter; has given lectures at educational symposiums organized by Baxter, Bayer, and Novo Nordisk; has received payment for lectures from Baxter, Bayer, and Novo Nordisk; and has received the Award from Baxter Coagulation Research Fund in Japan. K.F. and K.A. are professors of additional post in Molecular Genetics of Coagulation Disorder without additional salary. K.A. is a board member of the Factor Eight Inhibitor Bypass Activity Post Marketing Surveillance Study Board in Japan organized by Baxter; has received payment for lectures from Baxter, Bayer, Biogen Idec, Kaketsuken, Novo Nordisk, and Pfizer; has received payment for consultancy meetings with Baxter, Bayer, CSL Behring, Kaketsuken, Novo Nordisk, and Pfizer; and has received unrestricted grants supporting research from Pfizer. K.F. is an investigator of Hemophilia Research Study Update organized by Baxter, a board member of the Advate Safety Board in Japan organized by Baxter, and a board member of the Benefix Post Marketing Surveillance Study Board in Japan, organized by Pfizer; has received payment for consultancy meetings with Baxter, Pfizer, Biogen Idec, Bayer, CSL Behring, Kaketsuken, SRL, Mitsubishi Chemical Medience, and Novo Nordisk; has received unrestricted grants supporting research from Baxter, Pfizer, Bayer, Kaketsuken, Japan Blood Products Organization, and CSL Behring; and has received payment for lectures from Baxter, Bayer, Pfizer, Novo Nordisk, CSL Behring, Roche Diagnostics, Fujirebio Inc, and Sekisui Medical. M.S. is a board member of the Feiba and an Advate Safety Board in Japan, organized by Baxter, and a board member of the Benefix Post Marketing Surveillance Study Board in Japan, organized by Pfizer; has received payment for consultancy meetings with Baxter, Pfizer, Biogen Idec, Bayer, CSL Behring, Kaketsuken, Chugai Therapeutic Company, and Novo Nordisk; has received unrestricted grants supporting research from Baxter, Pfizer, Bayer, Kaketsuken, Novo Nordisk, Chugai

Pharmaceutical Company, and CSL Behring; and has received payment for lectures from Baxter, Bayer, Novo Nordisk, and Pfizer. The remaining authors declare no competing financial interests.

Correspondence: Keiji Nogami, Department of Pediatrics, Nara Medical University, Kashihara, Nara 634-8522, Japan; e-mail: roc-noga@naramed-u.ac.jp.

References

1. Dahlbäck B, Carlsson M, Svensson PJ. Familial thrombophilia due to a previously unrecognized mechanism characterized by poor anticoagulant response to activated protein C: prediction of a cofactor to activated protein C. *Proc Natl Acad Sci USA.* 1993;90(3):1004-1008.
2. Bertina RM, Koeleman BP, Koster T, et al. Mutation in blood coagulation factor V associated with resistance to activated protein C. *Nature.* 1994;369(6475):64-67.
3. Rosing J, Tans G. Coagulation factor V: an old star shines again. *Thromb Haemost.* 1997;78(1): 427-433.
4. Suzuki K, Dahlbäck B, Stenflo J. Thrombin-catalyzed activation of human coagulation factor V. *J Biol Chem.* 1982;257(11):6556-6564.
5. Foster WB, Nesheim ME, Mann KG. The factor Xa-catalyzed activation of factor V. *J Biol Chem.* 1983;258(22):13970-13977.
6. Walker FJ, Sexton PW, Esmon CT. The inhibition of blood coagulation by activated Protein C through the selective inactivation of activated Factor V. *Biochim Biophys Acta.* 1979;571(2): 333-342.
7. Suzuki K, Stenflo J, Dahlbäck B, Teodorsson B. Inactivation of human coagulation factor V by activated protein C. *J Biol Chem.* 1983;258(3): 1914-1920.
8. Nicolaes GA, Tans G, Thomassen MC, et al. Peptide bond cleavages and loss of functional activity during inactivation of factor Va and factor VaR506Q by activated protein C. *J Biol Chem.* 1995;270(36):21158-21166.
9. Gale AJ, Xu X, Pellequer JL, Getzoff ED, Griffin JH. Interdomain engineered disulfide bond permitting elucidation of mechanisms of inactivation of coagulation factor Va by activated protein C. *Protein Sci.* 2002;11(9):2091-2101.
10. Mann KG, Nesheim ME, Church WR, Haley P, Krishnaswamy S. Surface-dependent reactions of the vitamin K-dependent enzyme complexes. *Blood.* 1990;76(1):1-16.
11. Eaton D, Rodriguez H, Vehar GA. Proteolytic processing of human factor VIII. Correlation of specific cleavages by thrombin, factor Xa, and activated protein C with activation and inactivation of factor VIII coagulant activity. *Biochemistry.* 1986;25(2):505-512.
12. Fay PJ, Smudzin TM, Walker FJ. Activated protein C-catalyzed inactivation of human factor VIII and factor VIIIa. Identification of cleavage sites and correlation of proteolysis with cofactor activity. *J Biol Chem.* 1991;266(30):20139-20145.
13. Gale AJ, Cramer TJ, Rozenshteyn D, Cruz JR. Detailed mechanisms of the inactivation of factor VIIIa by activated protein C in the presence of its cofactors, protein S and factor V. *J Biol Chem.* 2008;283(24):16355-16362.
14. O'Brien LM, Mastri M, Fay PJ. Regulation of factor VIIIa by human activated protein C and protein S: inactivation of cofactor in the intrinsic factor Xase. *Blood.* 2000;95(5):1714-1720.
15. Thorelli E, Kaufman RJ, Dahlbäck B. The C-terminal region of the factor V B-domain is crucial for the anticoagulant activity of factor V. *J Biol Chem.* 1998;273(26):16140-16145.
16. Lu D, Kalafatis M, Mann KG, Long GL. Comparison of activated protein C/protein S-mediated inactivation of human factor VIII and factor V. *Blood.* 1996;87(11):4708-4717.
17. Rees DC, Cox M, Clegg JB. World distribution of factor V Leiden. *Lancet.* 1995;346(8983): 1133-1134.
18. Rees DC. The population genetics of factor V Leiden (Arg506Gln). *Br J Haematol.* 1996;95(4): 579-586.
19. Williamson D, Brown K, Luddington R, Baglin C, Baglin T. Factor V Cambridge: a new mutation (Arg306—>Thr) associated with resistance to activated protein C. *Blood.* 1998;91(4): 1140-1144.
20. Norstrøm E, Thorelli E, Dahlbäck B. Functional characterization of recombinant FV Hong Kong and FV Cambridge. *Blood.* 2002;100(2):524-530.
21. Chan WP, Lee CK, Kwong YL, Lam CK, Liang R. A novel mutation of Arg306 of factor V gene in Hong Kong Chinese. *Blood.* 1998;91(4): 1135-1139.
22. Nicolaes GA, Dahlbäck B. Factor V and thrombotic disease: description of a janus-faced protein. *Arterioscler Thromb Vasc Biol.* 2002; 22(4):530-538.
23. Foster PA, Fulcher CA, Houghten RA, de Graaf Mahoney S, Zimmerman TS. Localization of the binding regions of a murine monoclonal anti-factor VIII antibody and a human anti-factor VIII alloantibody, both of which inhibit factor VIII procoagulant activity, to amino acid residues threonine351-serine365 of the factor VIII heavy chain. *J Clin Invest.* 1988;82(1):123-128.
24. Mimms LT, Zampighi G, Nozaki Y, Tanford C, Reynolds JA. Phospholipid vesicle formation and transmembrane protein incorporation using octyl glucoside. *Biochemistry.* 1981;20(4):833-840.
25. Shinozawa K, Amano K, Suzuki T, et al. Molecular characterization of 3 factor V mutations, R2174L, V1813M, and a 5-bp deletion, that cause factor V deficiency. *Int J Hematol.* 2007;86(5):407-413.
26. Matsumoto T, Nogami K, Ogiwara K, Shima M. A modified thrombin generation test for investigating very low levels of factor VIII activity in hemophilia A. *Int J Hematol.* 2009;90(5):576-582.
27. Castoldi E, Brugge JM, Nicolaes GA, Girelli D, Tans G, Rosing J. Impaired APC cofactor activity of factor V plays a major role in the APC resistance associated with the factor V Leiden (R506Q) and R2 (H1299R) mutations. *Blood.* 2004;103(11):4173-4179.
28. Ortel TL, Devore-Carter D, Quinn-Allen M, Kane WH. Deletion analysis of recombinant human factor V. Evidence for a phosphatidylserine binding site in the second C-type domain. *J Biol Chem.* 1992;267(6):4189-4198.
29. Shen L, Dahlbäck B. Factor V and protein S as synergistic cofactors to activated protein C in degradation of factor VIIIa. *J Biol Chem.* 1994; 269(29):18735-18738.
30. Nogami K, Wakabayashi H, Schmidt K, Fay PJ. Altered interactions between the A1 and A2 subunits of factor VIIIa following cleavage of A1 subunit by factor Xa. *J Biol Chem.* 2003;278(3): 1634-1641.
31. Kamikura Y, Wada H, Yamada A, et al. Increased tissue factor pathway inhibitor in patients with acute myocardial infarction. *Am J Hematol.* 1997; 55(4):183-187.
32. Kalafatis M, Bertina RM, Rand MD, Mann KG. Characterization of the molecular defect in factor VR506Q. *J Biol Chem.* 1995;270(8):4053-4057.
33. Thorelli E, Kaufman RJ, Dahlbäck B. Cleavage of factor V at Arg 506 by activated protein C and the expression of anticoagulant activity of factor V. *Blood.* 1999;93(8):2552-2558.
34. Macedo-Ribeiro S, Bode W, Huber R, et al. Crystal structures of the membrane-binding C2 domain of human coagulation factor V. *Nature.* 1999;402(6760):434-439.
35. Saleh M, Peng W, Quinn-Allen MA, et al. The factor V C1 domain is involved in membrane binding: identification of functionally important amino acid residues within the C1 domain of factor V using alanine scanning mutagenesis. *Thromb Haemost.* 2004;91(1):16-27.
36. Adams TE, Hockin MF, Mann KG, Everse SJ. The crystal structure of activated protein C-inactivated bovine factor Va: Implications for cofactor function. *Proc Natl Acad Sci USA.* 2004;101(24): 8918-8923.
37. Fay PJ. Activation of factor VIII and mechanisms of cofactor action. *Blood Rev.* 2004;18(1):1-15.
38. Nogami K, Wakabayashi H, Fay PJ. Mechanisms of factor Xa-catalyzed cleavage of the factor VIIIa A1 subunit resulting in cofactor inactivation. *J Biol Chem.* 2003;278(19):16502-16509.
39. Duckers C, Simioni P, Spiezia L, et al. Residual platelet factor V ensures thrombin generation in patients with severe congenital factor V deficiency and mild bleeding symptoms. *Blood.* 2010;115(4): 879-886.
40. Mumford AD, McVey JH, Morse CV, et al. Factor V I359T: a novel mutation associated with thrombosis and resistance to activated protein C. *Br J Haematol.* 2003;123(3):496-501.
41. Zöller B, Svensson PJ, He X, Dahlbäck B. Identification of the same factor V gene mutation in 47 out of 50 thrombosis-prone families with inherited resistance to activated protein C. *J Clin Invest.* 1994;94(6):2521-2524.
42. Cai H, Hua B, Fan L, Wang Q, Wang S, Zhao Y. A novel mutation (g2172—>c) in the factor v gene in a chinese family with hereditary activated protein C resistance. *Thromb Res.* 2010;125(6): 545-548.

Journal of Thrombosis and Haemostasis, **12**: 355–362 DOI: 10.1111/jth.12488

ORIGINAL ARTICLE

Optimal monitoring of bypass therapy in hemophilia A patients with inhibitors by the use of clot waveform analysis

J. HAKU, K. NOGAMI, T. MATSUMOTO, K. OGIWARA and M. SHIMA
Department of Pediatrics, Nara Medical University, Kashihara, Nara, Japan

To cite this article: Haku J, Nogami K, Matsumoto T, Ogiwara K, Shima M. Optimal monitoring of bypass therapy in hemophilia A patients with inhibitors by the use of clot waveform analysis. *J Thromb Haemost* 2014; **12**: 355–62.

Summary. *Background:* Assays to determine the optimal hemostatic effects of bypass therapy in hemophilia A (HA) patients with inhibitors are difficult to compare. Clot waveform analysis (CWA), based on the continuous monitoring of routine coagulation parameters (prothrombin time/activated partial thromboplastin time), offers a useful method for assessing global clotting function. *Objectives:* To investigate the technique of CWA for the hemostatic monitoring of bypass therapy in HA patients with inhibitors. *Methods and Results:* Ellagic acid (Elg), tissue factor (TF) or both (Elg/TF) were used as trigger reagents in CWA. The standard parameters – clot time (CT), maximum coagulation velocity (|min1|), and acceleration (|min2|) – were recorded. Optimal monitoring was defined as: (i) a significant difference in these parameters between plasma from HA patients with inhibitors and normal plasmas; and (ii) a significant improvement in these indices in HA patients with inhibitors after bypass therapy. Experiments *in vitro* demonstrated that there were significant differences between plasma from HA patients with inhibitors and normal plasma with various triggers, in the order Elg > Elg/TF >> TF. Addition of therapeutically achievable concentrations of bypassing agents, however, showed significant improvements in the different parameters only with Elg/TF, suggesting that this reagent provided the most appropriate assay. A total of 20 plasmas from HA patients with inhibitors in which bypassing agents were infused were evaluated *ex vivo* by Elg/TF CWA. The postinfusion parameters CT and |min2| reflected clinical effects, and were close to normal levels. Furthermore, Elg/TF CWA facilitated quantitative evaluation of perioperative hemostatic management of bypass therapy in HA patients with inhibitors. *Conclusions:* CWA is a promising method for the quantitative monitoring of bypass therapy during routine automated clotting assays with a modified trigger reagent comprising a well-balanced mixture of Elg and TF.

Keywords: blood coagulation factor inhibitors; clinical laboratory techniques; factor VIII; hemophilia A; hemostatic techniques.

Correspondence: Keiji Nogami, Department of Pediatrics, Nara Medical University, 840 Shijo-cho, Kashihara, Nara 634-8522, Japan.
Tel.: +81 744 29 8881; fax +81 744 24 9222.
E-mail: roc-noga@naramed-u.ac.jp

An account of this work was presented at the 54th annual meeting of the American Society of Hematology, Atlanta, GA, USA, 10 December 2012.

Received 21 August 2013
Manuscript handled by: M. Levi
Final decision: P. H. Reitsma, 7 December 2013

Introduction

Hemophilia A (HA) results from a deficiency or defect of the coagulant protein factor VIII, and is the most common of the severe, inherited bleeding disorders. Treatment for HA patients has markedly improved over recent years, but the development of FVIII inhibitor alloantibodies in 20–30% of multitransfused patients with severe HA remains a serious clinical problem [1]. Bypassing agents, utilizing activated prothrombin complex concentrates (activated prothrombin complex concentrate [APCC]; FEIBA) and recombinant FVIIa (rFVIIa) (NovoSeven) are now used for the treatment of HA patients with inhibitors, especially those classed as high responders. In HA patients without inhibitors, there is a close relationship between clinical severity and the level of FVIII activity (FVIII:C) measured with one-stage clotting assays, whereas in HA patients with inhibitors there is no such relationship, and the levels of FVIII in plasma samples after treatment with FVIII concentrates remain undetectable. Furthermore, it is difficult to determine the optimum effects of bypass therapy in these patients, and no single assay has been shown to effectively monitor this type of treatment.

Laboratory methods to monitor the use of bypassing agents in HA patients with inhibitors are currently being widely investigated, in order to assess effective therapeutic

doses, and to enable the clinical management of hemostatic responses and thrombotic risks associated with treatment. In this respect, simple and rapid assays appear to be essential, given that patients frequently represent medical emergencies. A number of techniques based on the measurement of global coagulation function have been developed for this purpose, in particular thromboelastography and the thrombin generation test (TGT) [2]. Rotational thromboelastometry (ROTEM) [3] utilizes whole blood, and requires analysis within a restricted time scale. This method also appears to have high variability, not only between subjects but also within the same subject [4]. The calibrated automated TGT provides a measure of overall coagulation, and the results have been shown to correlate with both hemorrhagic and thrombotic states [5]. Moreover, the method has been suggested as a possible means to monitor the hemostatic effects of bypass therapy [6,7]. The procedure is complicated, however, and the concentration of tissue factor (TF) used to initiate coagulation in the assay significantly influences its sensitivity to individual coagulation factors [8,9]. Soluble ellagic acid (Elg), an activator of intrinsic coagulation in an activated partial thromboplastin time (APTT)-based assay, also provides a sensitive index of coagulation function in the TGT. We recently reported that thrombin generation initiated by a mixture of Elg and TF at low concentrations enabled us to classify clinical severity in HA patients with lower levels of FVIII:C [10], reflecting the activation of both intrinsic and extrinsic pathways based on the cell-based coagulation model.

Clot waveform analysis (CWA) is a more recently developed global coagulation assay. CWA is based on the continuous observation of the changes in light transmittance that occur as fibrin is formed in plasma during the performance of routine clotting tests, such as the APTT assay and the prothrombin time assay [11]. The data obtained from this assay reflect the overall process of hemostasis, including fibrinolytic activity. Shima *et al.* have demonstrated that there are several advantages to the use of CWA in HA patients without inhibitors [12,13]. In addition, recommendations on the standardization and clinical application of this assay have recently been reported by the Scientific and Standardization Committee of the ISTH [14]. In the present study, we attempted to optimize CWA for the hemostatic monitoring of bypass therapy in HA patients with inhibitors.

Materials and methods

Reagents

Bypassing agents – rFVIIa (NovoSeven) and APCC (FEIBA) – were kindly provided by Novo Nordisk (Bagsværd, Denmark) and Baxter Japan (Tokyo, Japan), respectively. Recombinant human TF (Innovin; Dade, Marburg, Germany) and Elg (Sysmex, Kobe, Japan) were purchased from the indicated vendors. Phospholipid (PL) vesicles containing 10% phosphatidylserine, 60% phosphatidylcholine and 30% phosphatidylethanolamine were prepared as previously described [15]. Congenital FVIII-deficient plasmas were purchased from George King Bio-Medical (Overland Park, KS, USA).

Plasma samples

Normal pooled plasmas were prepared from 30 normal healthy individuals. Blood was drawn into evacuated anticoagulant tubes containing a 1 : 9 volume of 3.8% (w/v) trisodium citrate. After centrifugation for 15 min at 1500 × *g*, the plasmas were stored at − 80 °C, and thawed at 37 °C immediately prior to the assays. Patients' plasmas were obtained from seven HA patients with inhibitors. Blood samples were obtained from patients diagnosed by our research group and enrolled in the Nara Medical University Hemophilia Program. All samples were obtained after informed consent had been obtained, following local ethical guidelines.

CWA

CWA was performed on the MDA-II system (Trinity Biotech, Dublin, Ireland), with various trigger reagents and minor modifications of previous methods [13]. FVIII-deficient plasmas or HA plasmas with inhibitors were mixed with various concentrations of bypassing agents (rFVIIa or APCC) and various trigger reagents. Clinically therapeutic doses of rFVIIa (90 μg kg^{-1}) and APCC (80 IU kg^{-1}) correspond to 25 nM and ~ 1 IU mL^{-1} in circulating blood, respectively. On the basis of the results of our previously described TGT optimized for assessing global coagulation in HA [10], three trigger reagents were used: (i) Elg trigger – Elg (0.3 μM) and PL (10 μM); (ii) TF trigger – TF (0.1 pM) and PL (10 μM); and (iii) Elg/TF – Elg (0.3 μM), TF (0.1 pM), and PL (10 μM). Clot formation was initiated by the addition of $CaCl_2$ (20 mM). The clot waveforms obtained were computer-processed with the commercial kinetic algorithm. The minimum value of the first derivative (min1) was calculated as an indicator of the maximum velocity of coagulation achieved. The second derivative of the transmittance data reflected the acceleration of the reaction at any given time point. The minimum value of the second derivative (min2) was calculated as an index of the maximum acceleration of the reaction achieved. As the minima of min1 and min2 were derived from negative changes, the data were expressed as |min1| and |min2|, respectively. The clot time (CT) was defined as the time until the start of coagulation.

ROTEM

ROTEM was performed with the Whole Blood Hemostasis Analyzer (Pentapharm, Munich, Germany). After

being drawn, citrated whole blood was kept at rest for 30 min at room temperature, and was used within 2 h. At the start of measurement, 20 μL of $CaCl_2$ (final concentration, 12.5 mM) was added to the whole blood (280 μL).

Results

Clot waveforms of FVIII-deficient plasma in the presence of bypassing agents

We first examined the changes in clot waveforms with FVIII-deficient plasma (HA) after the addition of individual bypassing agents (rFVIIa or APCC) *in vitro*. Various concentrations of rFVIIa or APCC were added to FVIII-deficient plasma in the presence of the three different trigger reagents (Elg, TF, or Elg/TF), as described in Materials and methods. Figure 1A shows the clot waveforms observed after the addition of rFVIIa. In the present study, we defined improvement in hemostatic effect as improvement in laboratory assessment findings showing good clinical hemostasis. The clot waveforms observed with Elg or TF trigger in the absence of rFVIIa showed maximum or minimum differences, respectively, between FVIII-deficient plasma and normal plasma. With the combined Elg/TF trigger, an intermediate difference between these samples was observed. With the addition of rFVIIa, dose-dependent improvements in clot waveforms were recorded with all of the trigger reagents. At a clinically therapeutic concentration of rFVIIa (25 nM) in the presence of the Elg trigger, the FVIII-deficient waveform data appeared to remain unsatisfactory. In contrast, with the TF trigger, even small amounts of rFVIIa (0.2 nM) added to FVIII-deficient plasma resulted in waveform changes that suggested a hypercoagulant state beyond that seen with normal plasma. With the Elg/TF trigger at this therapeutic level of rFVIIa, however, FVIII-deficient waveforms seemed to be closer to normal than those recorded with the Elg trigger.

Similar experiments were repeated after the addition of APCC (Fig. 1B), and, as above, dose-dependent improvements in waveforms were observed with all three trigger reagents. As with rFVIIa, the results with the TF trigger indicated that low concentrations of APCC (0.125 IU mL^{-1}) added to FVIII-deficient plasma could indicate a markedly hypercoagulant state relative to that seen with normal plasma. Moreover, again as above, FVIII-deficient clot waveforms obtained with the Elg trigger remained significantly defective as compared with normal plasma, even at high concentrations of APCC (2 IU mL^{-1}). With the Elg/TF trigger at therapeutic concentrations of APCC (1 IU mL^{-1}), however, the FVIII-deficient clot waveforms were close to those obtained with normal plasma, and at 2 IU mL^{-1} the results pointed to potential hypercoagulation. Overall, therefore, the single TF trigger seemed to overestimate the hemostatic activity

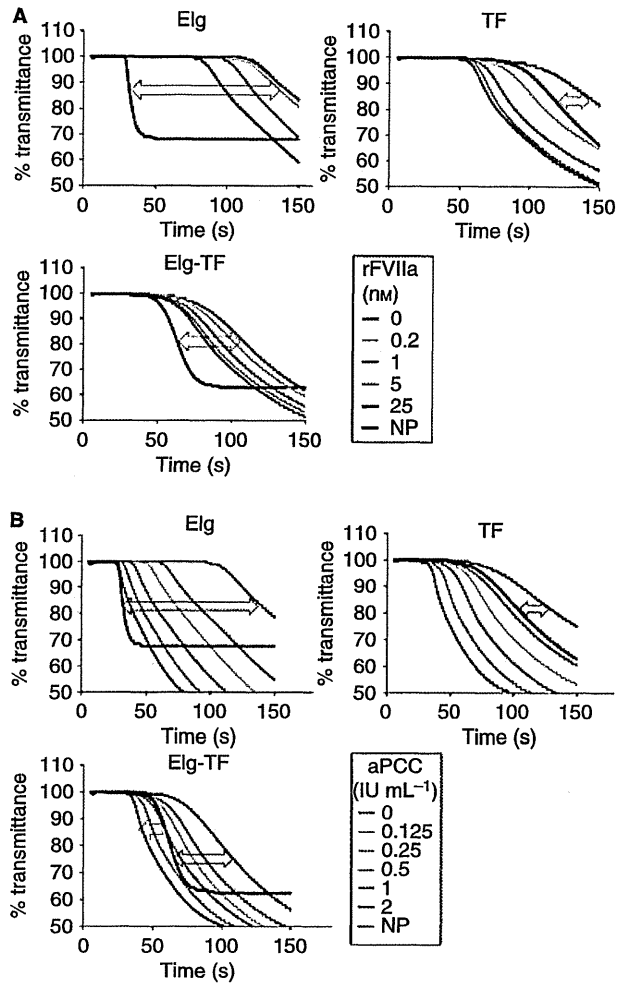

Fig. 1. Clot waveform analysis on the addition of bypassing agents to FVIII-deficient plasma. FVIII-deficient plasmas were mixed with various concentrations of recombinant FVIIa (rFVIIa) (0–25 nM [A]) or activated prothrombin complex concentrate (APCC) (0–2 IU mL^{-1} [B]) in the presence of each trigger reagent (ellagic acid [Elg], tissue factor [TF], or Elg/TF), and this was followed by the addition of $CaCl_2$ as described in Materials and methods. Clot waveforms were visualized, and representative data are illustrated. NP, normal control plasma. Black arrows indicate the difference between clot waveforms observed with NP and with FVIII-deficient plasma, and the red arrow indicates the difference between clot waveforms observed with NP and with FVIII-deficient plasma with added APCC (2 IU mL^{-1}).

of bypassing agents, whereas the Elg trigger alone appeared to inadequately reflect coagulation potential. The findings suggested that use of the combined Elg/TF reagent in CWA provided the most appropriate data for monitoring the hemostatic effects of these therapeutic materials.

Quantitative monitoring of bypass therapy with the Elg/TF trigger in CWA

Two main aspects were considered regarding the use of CWA in the quantitative assessment of bypass therapy in

HA. First, results should clearly identify any significant differences between FVIII-deficient plasma and normal plasma; and second, the data should reflect significant improvements in the presence of a clinically therapeutic dose of rFVIIa (25 nM) or APCC (1 IU mL^{-1}). The parameters (CT, |min1|, and |min2|) calculated from the waveforms shown in Fig. 1 are summarized in Table 1. The data are expressed as the percentage difference between FVIII-deficient and normal plasma (percentage of control) after the addition of rFVIIa or APCC. In the absence of bypassing agent (buffer), the Elg and Elg/TF trigger parameters were significantly different. The TF trigger parameters were very close to control values, however, reflecting the inadequacy of this TF-only assay. In contrast, with the addition of a clinically therapeutic dose of rFVIIa (25 nM) or APCC (1 IU mL^{-1}), CT values obtained with both the Elg trigger and the Elg/TF trigger appeared to improve similarly as in normal plasma, whereas the improvements of |min1| and |min2| with the single Elg trigger were significantly less than those with the Elg/TF trigger. These *in vitro* experiments suggested that CWA with the Elg/TF trigger better reflected the hemostatic effects of bypass therapy than CWA with the separate reagents, and could be useful for the quantitative monitoring of treatment in HA patients with inhibitors.

Table 1 Parameters obtained in clot waveform analysis with ellagic acid (Elg), tissue factor (TF) and Elg/TF triggers in FVIII-deficient plasma with bypassing agents

	CT			|min1|			|min2|		
Samples	Elg	TF	Elg/TF	Elg	TF	Elg/TF	Elg	TF	Elg/TF
FVIII-deficient plasma									
+ Buffer	372	86	147	16	90	33	13	119	21
+ 25 nM rFVIIa	271	48	100	20	175	54	18	317	47
+ 1 IU mL^{-1} APCC	122	33	69	27	220	69	32	448	71

APCC, activated prothrombin complex concentrate; CT, clot time; rFVIIa, recombinant factor FVIIa. The data are expressed as the percentage difference between FVIII-deficient and normal plasma (% of control).

Assessment of CWA with the Elg/TF trigger in vivo

The hemostatic effects of rFVIIa (~ 25 nM) or APCC (~ 1 IU mL^{-1}) in HA patients with inhibitors were also assessed *in vivo*. For hemostatic management, because we needed the full dose per unit time of rFVIIa or APCC for HA patients with inhibitors during surgical procedures, we performed CWA with the administration of single dose of bypassing agent. A total of 20 samples from seven patients were examined (seven preinfusion and postinfusion samples for rFVIIa, and three preinfusion and postinfusion samples for APCC; Table 2). Significant improvements in symptoms were observed in six patients, and the ROTEM data in these instances were in keeping with the clinical responses. Therapy with rFVIIa in case 7 appeared to be clinically ineffective, however, although there were good improvements in the ROTEM results. Three of the patients treated with rFVIIa were also treated with APCC (cases 1–3).

Plasma samples from these patients before and after infusion of bypassing agents were also studied with CWA, as described above. Representative clot waveforms obtained with the Elg/TF trigger are shown in Fig. 2. Postinfusion samples were taken 30 min after treatment. Plasma samples for cases 1–3 were obtained after individual infusion of rFVIIa and APCC during the same procedure. In three cases, the effect of rFVIIa infusion was first examined with CWA, and that of APCC infusion

Table 2 Hemophilia A patients with inhibitors on bypass therapy with recombinant factor VIIa (rFVIIa) or activated prothrombin complex concentrate (APCC). (i) rFVIIa infusion; (ii) APCC infusion

Case	Age (years)	Inhibitor (BU mL^{-1})	Operation	Dose (μg kg^{-1})	Clinical effect	ROTEM
(i)						
1	9	12	Implantation of CV port	90	Good	Good
2	23	49	Implantation of CV port	125	Good	Good
3	48	25	Synovectomy	90	Good	Good
4	18	56	Exodontia	104	Good	Good
5	9	20	Synovectomy	120	Good	Good
6	10	59	Synovectomy	105	Good	Good
7	9	12	Synovectomy	90	Poor	Good
(ii)						
1	9	12	Implantation of CV port	90	Good	Good
2	23	49	Implantation of CV port	125	Good	Good
3	48	25	Synovectomy	90	Good	Good

BU, Bethesda unit; CV port, central venous port; ROTEM, rotational thromboelastometry. Cases 1–3 in rFVIIa infusion are same patients to those in APCC infusion. Samples for cases 1–3 were obtained with the individual administration of bypassing agents during the same procedure as described in Results.

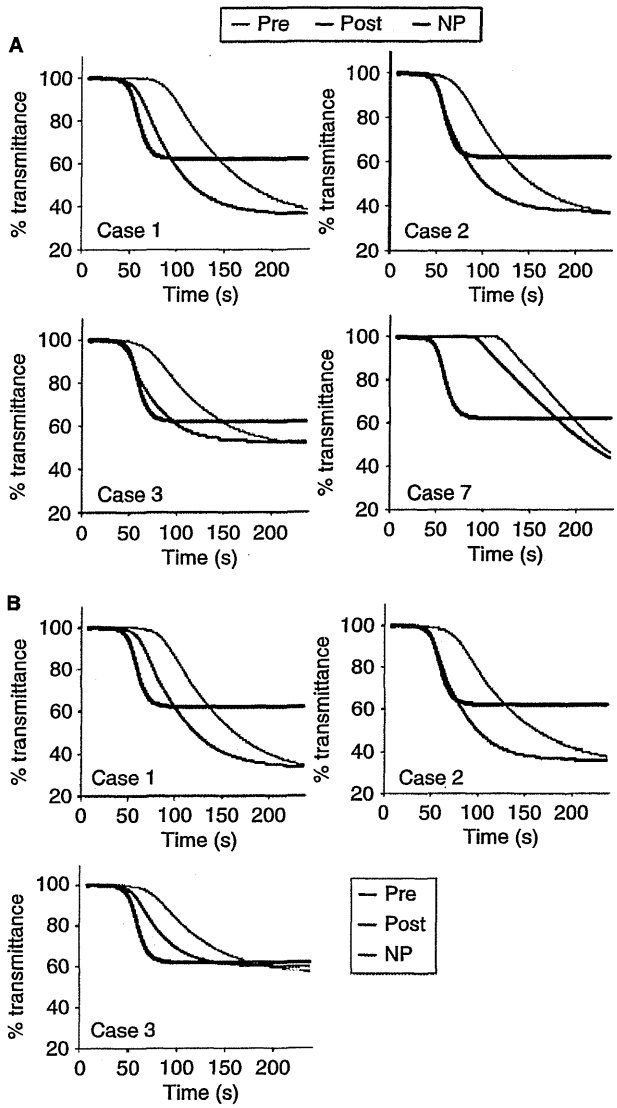

Fig. 2. Clot waveform analysis on the infusion of recombinant FVIIa (rFVIIa) or activated prothrombin complex concentrate (APCC) for hemophilia A patients with inhibitors. Patients' plasma samples, obtained before or after infusion of rFVIIa (A) or APCC (B), were mixed with the ellagic acid/tissue factor trigger reagent, and this was followed by the addition of $CaCl_2$. Clot waveforms were visualized, and representative data are illustrated. NP, normal control plasma.

was further studied after 24 h of rFVIIa infusion. The effect of rFVIIa completely disappeared in CWA at 24 h postinfusion, and did not affect that of APCC (data not shown). Near or complete normalization of clot waveforms was apparent after infusion of rFVIIa (Fig. 2A) and APCC (Fig. 2B). Similar patterns were found in the other cases (data not shown). In case 7, however, the clot waveforms after infusion of rFVIIa remained significantly defective (Fig. 2A), consistent with the lack of clinical effect, and unlike what was found with ROTEM.

The parameters (CT and |min2|) derived from the clot waveforms preinfusion and postinfusion were quantified as the percentage difference between patient and normal plasma (percentage of control), as described above for the experiments *in vitro*. The results are shown in Fig. 3 (Fig. 3A; rFVIIa; Fig. 3B; APCC). The CT values improved to normal levels, and significant enhancements in |min2| were demonstrated (2–4.5-fold increase). In case 7, however, these calculated figures emphasized the clot waveform patterns, and were in keeping with the poor clinical effects of therapy (preinfusion/postinfusion, CT and |min2|, 184%/148% and 37%/39% of control, respectively). These quantitative data confirmed that CWA with the Elg/TF trigger gave a good reflection of the hemostatic effects of rFVIIa and APCC in HA patients with inhibitors.

Perioperative management of therapy with rFVIIa by use of CWA with the Elg/TF trigger

Treatment with rFVIIa was monitored with CWA with the Elg/TF trigger in two surgical cases (cases 1 and 2). In both patients, the surgical procedures involved implantation of central venous ports. The CT and |min2| values were recorded from samples obtained before and after infusion of rFVIIa during the perioperative period. Clinically effective hemostatic management was achieved in both cases, and the postoperative CT and |min2| results remained close to and within the normal range (Fig. 4A, B). These results confirmed that CWA with the Elg/TF trigger reflected the hemostatic effects of bypass therapy in HA patients with inhibitors, and could provide useful data for the perioperative monitoring of treatment during surgery.

Discussion

We have investigated the use of CWA for monitoring hemostasis in HA patients with inhibitors treated with rFVIIa and APCC, and have demonstrated a good correlation between the changes in clot waveforms and the hemostatic effects of the bypassing agents. In particular, the clot waveforms, together with the specific parameters derived from CWA, improved significantly, and were close to the normal levels observed with concentrations of rFVIIa (25 nM) and APCC (1 U mL^{-1}) that are believed to represent clinically therapeutic doses. The most appropriate CWA technique appeared to be that with a trigger comprising a mixture of Elg and TF rather than individual initiating reagents. Furthermore, low concentrations of TF (0.1 pM) and Elg (0.3 μM) enabled the monitoring of hemostatic effects of rFVIIa and APCC both *ex vivo* and *in vivo*. In addition, the use of this method helped with successful perioperative hemostatic management in two patients treated with rFVIIa. Our findings therefore demonstrate that a trigger reagent containing a well-balanced mixture of Elg and TF in

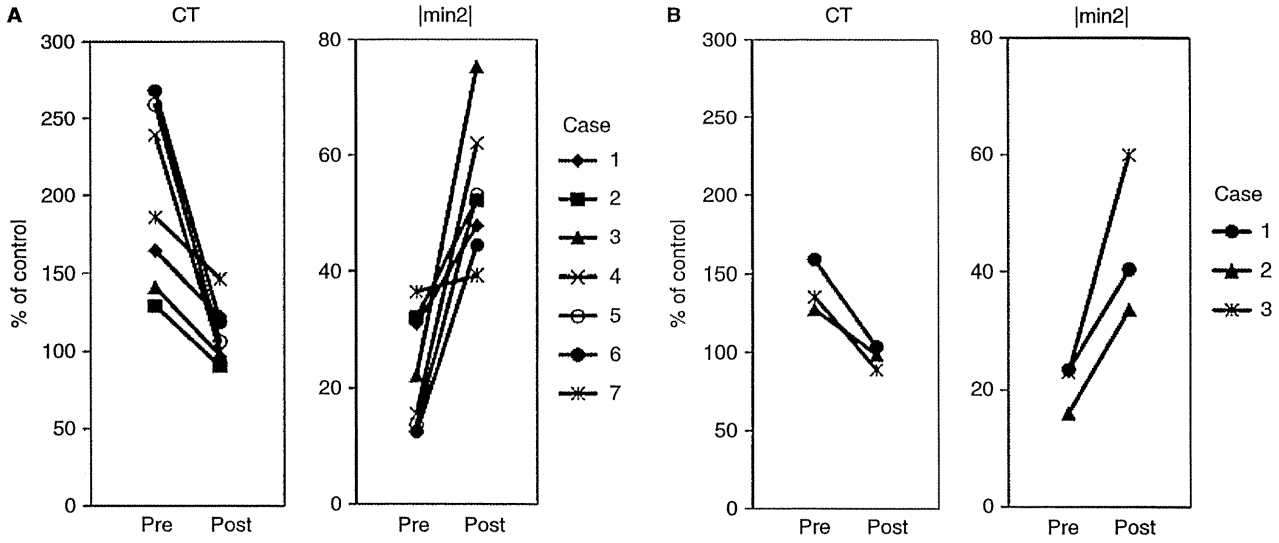

Fig. 3. Clot waveform analysis (CWA) parameters in hemophilia A patients with inhibitors who were infused with recombinant FVIIa (rFVIIa) or activated prothrombin complex concentrate (APCC). Patients' plasma samples, before or after infusion of rFVIIa (A) or APCC (B), were analyzed with CWA with the ellagic acid/tissue factor trigger. Parameters (clot time [CT] and minimum value of the second derivative [|min2|]) obtained preinfusion and postinfusion are shown. Parameters obtained with normal plasma were regarded as 100%.

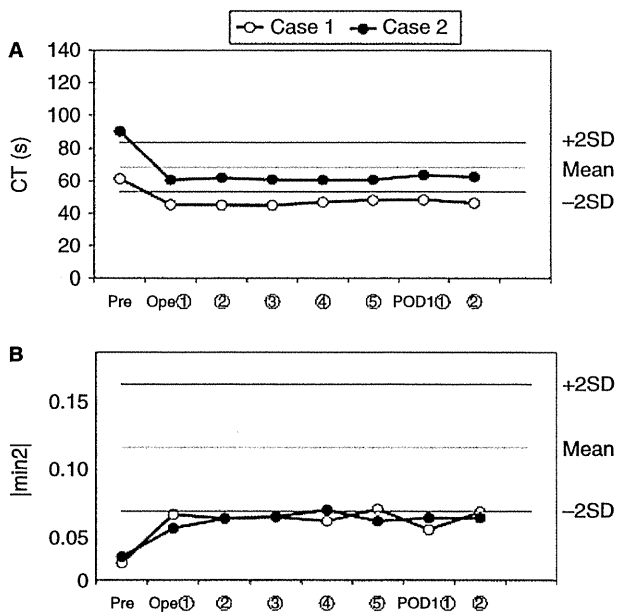

Fig. 4. Clot waveform analysis (CWA) parameters for perioperative hemostatic management with infusion of recombinant FVIIa (rFVIIa) in two cases. Patients' plasmas (cases 1 and 2) were obtained before or after infusion of rFVIIa during perioperative management, and were analyzed with CWA with the ellagic acid/tissue factor trigger. Parameters (clot time [CT] [A] and minimum value of the second derivative [|min2|] [B]) preinfusion or postinfusion are shown. The straight horizontal lines represent the mean ± 2 SD of normal plasmas. Ope, operation; POD1, postoperative day 1; SD, standard deviation.

CWA could provide a promising assay for the quantitative assessment of bypass therapy in HA patients with inhibitors.

Previous studies have generally utilized the TGT with the TF trigger to evaluate FVIII replacement therapy in HA. Variable TGT parameters are often observed in HA patients with similar levels of FVIII:C, and different ranges of endogenous thrombin potential (ETP) have been demonstrated even in normal individuals [10]. Our earlier investigations centered on the use of the TGT to identify clinical differences in patients with very low levels of FVIII:C. We established a modified TGT incorporating Elg/TF (initiating both the intrinsic and extrinsic pathways) to initiate thrombin generation, and the method appeared to accurately reflect coagulation function in this complex group of HA patients [10]. We chose Elg for the following reasons: (i) in the TGT, the Elg trigger provided similar results to the FIXa trigger (data not shown); (ii) coagulation disorders other than HA can also be evaluated; and (iii) it is stable in solution and cost-effective. In the current studies, we similarly found that it was difficult to assess the clinical properties of bypassing agents with Elg or TF alone to initiate reactions in the CWA, but the mixed reagent (Elg/TF), promoting both the intrinsic and extrinsic coagulation pathways, provided data that demonstrated a good correlation between laboratory parameters and clinical status. The use of low concentrations of TF has been reported to improve the capability of the TGT [9,16], and our findings indicate that this could also be true for CWA. We observed that high concentrations of TF were not satisfactory for monitoring hemostasis (data not shown). In addition, there appeared to be a major discrepancy between the results of ROTEM and those of Elg/TF CWA after therapy with rFVIIa (case 7). One reason for this discrepancy may be the use of whole blood in ROTEM, but the

precise reason remains unknown. Together, these findings suggest that the waveform technique is more sensitive to hemostasis mechanisms *in vivo*.

Treatment of HA patients with high-responding inhibitors remains a major challenge, especially in cases of life-threatening bleeding or major surgery. Neither practical guidelines for optimal therapy with bypassing agents nor standards for hemostatic monitoring have been defined, although the use of the TGT or ROTEM has been reported recently for this purpose. In particular, Dargaud *et al.* have studied the application of the TGT in surgical settings, and have shown that prospective clinical assessment with this assay might be useful in selecting the most effective therapeutic options in HA patients with inhibitors [7,17]. However, the sensitivity and specificity of the TGT for individual coagulation factors depends on the TF concentration [9,16]. The results appear to be variable, and assays performed in different conditions do not always correlate. In addition, the TGT is technically more complicated than CWA. ROTEM requires the use of whole blood samples, and has been found to have high variability, not only between subjects but also within the same subject. The consensus appears to be that this method is too unreliable for routine monitoring [4]. In contrast, CWA can be simply performed with plasma, and enables assessment of APCC and rFVIIa therapy with similar sensitivity. The technique could also help to identify a hypercoagulant state. At present, not all coagulation analyzers can be used for CWA, but the number of appropriate analyzers is increasing [14], and the application of CWA is being extended. In this context, we have recently used CWA to evaluate the apparent differences in coagulation function between patients with acquired HA and those with congenital HA [18].

Previous reports on the use of the TF TGT for monitoring FVIII therapy in HA have suggested that measurements of ETP might provide a satisfactory index of hemostasis in HA patients with inhibitors [19,20]. The ETP appears to have low sensitivity, however, and we have found that results obtained with the TGT (in particular, ETP) do not correlate with lower levels of FVIII:C [10]. In contrast, CWA parameters seemed to provide a better correlation between clinical symptoms and very low levels of FVIII:C [13]. In the present study, we have demonstrated that the CWA parameters (CT, |min1|, and |min2|) can provide very useful quantitative information for the monitoring of hemostasis during treatment with rFVIIa and APCC, and for the perioperative management of this type of inhibitor-bypassing therapy.

In conclusion, we have reported a sensitive CWA assay for monitoring bypass therapy in HA patients with inhibitors as a first trial, although the number of cases in this study was small. At present, the method utilizes high-spun, platelet-poor plasma, and might not fully reflect physiologic hemostasis. Further studies are in progress to examine similar assays with alternative blood samples, including standardized, platelet-rich plasma. Recently, the standardization recommendations for clinical applications of CWA have been published [14], and the number of appropriate analyzers for CWA has been increasing. In order for monitoring with CWA to be used widely, the assessment and standardization of parameters obtained with a combination of different instruments and trigger reagents, and multicenter large studies including the hemostatic monitoring of surgery, will be required in future.

Addendum

J. Haku performed experiments and wrote the paper. K. Nogami designed the research, interpreted the data, and wrote the paper. T. Matsumoto, K. Ogiwara, and M. Shima interpreted the data.

Acknowledgements

This work was partly supported by grant MEXT KAKENHI 24591558 (K. Nogami).

Disclosure of Conflict of Interests

The authors state that they have no conflict of interest.

References

1 Oldenburg J, Brackmann HH, Schwaab R. Risk factors for inhibitor development in hemophilia A. *Haemotologica* 2000; **85**: 7–13.
2 Hemker HC. The mode of action of heparin in plasma. In: Verstraete M, Vermylen J, Lijnen R, Arnout J, eds. *Thrombosis and Haemostasis*. Leuven: Leuven University Press, 1987: 17–36.
3 Sørensen B, Johansen P, Christiansen K, Woelke M, Ingerslev J. Whole blood coagulation thrombelastographic profiles employing minimal tissue factor activation. *J Thromb Haemost* 2003; **1**: 551–8.
4 Kenet G, Stenmo CB, Blemings A, Wegert W, Goudemand J, Krause M, Schramm W, Kirchmaier C, Martinowitz U. Intrapatient variability of thromboelastographic parameters following in vivo and ex vivo administration of recombinant activated factor VII in haemophilia patients. A multi-centre, randomised trial. *Thromb Haemost* 2010; **103**: 351–9.
5 Hemker HC, Giesen P, Al Dieri R, Regnault V, de Smedt E, Wagenvoord R, Lecompte T, Béguin S. Calibrated automated thrombin generation measurement in clotting plasma. *Pathophysiol Haemost Thromb* 2003; **33**: 4–15.
6 Turecek PL, Váradi K, Keil B, Negrier C, Berntorp E, Astermark J, Bordet JC, Morfini M, Linari S, Schwarz HP. Factor VIII inhibitor-bypassing agents act by inducing thrombin generation and can be monitored by a thrombin generation assay. *Pathophysiol Haemost Thromb* 2003; **33**: 16–22.
7 Dargaud Y, Lienhart A, Meunier S, Hequet O, Chavanne H, Chamouard V, Marin S, Negrier C. Major surgery in a severe haemophilia A patient with high titre inhibitor: use of the thrombin generation test in the therapeutic decision. *Haemophilia* 2005; **11**: 552–8.
8 Keularts IM, Zivelin A, Seligsohn U, Hemker HC, Béguin S. The role of factor XI in thrombin generation induced by low concentrations of tissue factor. *Thromb Haemost* 2001; **85**: 1060–5.
9 van Veen JJ, Gatt A, Cooper PC, Kitchen S, Bowyer AE, Makris M. Corn trypsin inhibitor in fluorogenic thrombin-

generation measurements is only necessary at low tissue factor concentrations and influences the relationship between factor VIII coagulant activity and thrombogram parameters. *Blood Coagul Fibrinolysis* 2008; **19**: 183–9.

10 Matsumoto T, Nogami K, Ogiwara K, Shima M. A modified thrombin generation test for investigating very low levels of factor VIII activity in hemophilia A. *Int J Hematol* 2009; **90**: 576–82.

11 Braun PJ, Givens TB, Stead AG, Beck LR, Gooch SA, Swan RJ, Fischer TJ. Properties of optical data from activated partial thromboplastin time and prothrombin time assays. *Thromb Haemost* 1997; **78**: 1079–87.

12 Shima M, Matsumoto T, Fukuda K, Kubota Y, Tanaka I, Nishiya K, Giles AR, Yoshioka A. The utility of activated partial thromboplastin time (aPTT) clot waveform analysis in the investigation of hemophilia A patients with very low levels of factor VIII activity (FVIII:C). *Thromb Haemost* 2002; **87**: 436–41.

13 Matsumoto T, Shima M, Takeyama M, Yoshida K, Tanaka I, Sakurai Y, Giles AR, Yoshioka A. The measurement of low levels of factor VIII or factor IX in hemophilia A and hemophilia B plasma by clot waveform analysis and thrombin generation assay. *J Thromb Haemost* 2006; **4**: 377–84.

14 Shima M, Thachil J, Nair SC, Srivastava A. Towards standardization of the clot waveform analysis and recommendations for its clinical applications. *J Thromb Haemost* 2013; **11**: 1417–20.

15 Mimms LT, Zampighi G, Nozaki Y, Tanford C, Reynolds JA. Phospholipid vesicle formation and transmembrane protein incorporation using octyl glucoside. *Biochemistry* 1981; **20**: 833–40.

16 van Veen JJ, Gatt A, Bowyer AE, Cooper PC, Kitchen S, Makris M. The effect of tissue factor concentration on calibrated automated thrombography in the presence of inhibitor bypass agents. *Int J Lab Hematol* 2009; **31**: 189–98.

17 Dargaud Y, Lienhart A, Negrier C. Prospective assessment of thrombin generation test for dose monitoring of bypassing therapy in hemophilia patients with inhibitors undergoing elective surgery. *Blood* 2010; **116**: 5734–7.

18 Matsumoto T, Nogami K, Ogiwara K, Shima M. A putative inhibitory mechanism in the tenase complex responsible for loss of coagulation function in acquired haemophilia A patients with anti-C2 autoantibodies. *Thromb Haemost* 2012; **107**: 288–301.

19 Hemker HC, Béguin S. Phenotyping the clotting system. *Thromb Haemost* 2000; **84**: 747–51.

20 Dargaud Y, Béguin S, Lienhart A, Al Dieri R, Trzeciak C, Bordet JC, Hemker HC, Negrier C. Evaluation of thrombin generating capacity in plasma from patients with haemophilia A and B. *Thromb Haemost* 2005; **93**: 475–80.

Vaccine 32 (2014) 839–845

Contents lists available at ScienceDirect

Vaccine

journal homepage: www.elsevier.com/locate/vaccine

Effects of different promoters on the virulence and immunogenicity of a HIV-1 Env-expressing recombinant vaccinia vaccine

Mao Isshiki[a], Xianfeng Zhang[a,*], Hirotaka Sato[a,1], Takashi Ohashi[a], Makoto Inoue[b], Hisatoshi Shida[a]

[a] Institute for Genetic Medicine, Hokkaido University, Kita-ku, Sapporo 060-0815, Japan
[b] DNAVEC Corporation, Techno Park Oho, 6 Ohkubo, Tsukuba, Ibaraki 300-2611, Japan

ARTICLE INFO

Article history:
Received 2 October 2013
Received in revised form 5 December 2013
Accepted 10 December 2013
Available online 24 December 2013

Keywords:
LC16m8Δ
Promoter pSFJ1-10
Promoter p7.5
HIV-1 Env
Immunogenicity
Safety

ABSTRACT

Previously, we developed a vaccination regimen that involves priming with recombinant vaccinia virus LC16m8Δ (rm8Δ) strain followed by boosting with a Sendai virus-containing vector. This protocol induced both humoral and cellular immune responses against the HIV-1 envelope protein. The current study aims to optimize this regimen by comparing the immunogenicity and safety of two rm8Δ strains that express HIV-1 Env under the control of a moderate promoter, p7.5, or a strong promoter, pSFJ1-10. m8Δ-p7.5-JRCSFenv synthesized less gp160 but showed significantly higher growth potential than m8Δ-pSFJ-JRCSFenv. The two different rm8Δ strains induced antigen-specific immunity; however, m8Δ-pSFJ-JRCSFenv elicited a stronger anti-Env antibody response whereas m8Δ-p7.5-JRCSFenv induced a stronger Env-specific cytotoxic T lymphocyte response. Both strains were less virulent than the parental m8Δ strain, suggesting that they would be safe for use in humans. These findings indicate the vaccine can be optimized to induce favorable immune responses (either cellular or humoral), and forms the basis for the rational design of an AIDS vaccine using recombinant vaccinia as the delivery vector.

1. Introduction

Despite the increasing availability and effectiveness of antiretroviral treatments, a safe and effective vaccine that prevents HIV-1 infection would be invaluable. A recent report from Thailand showed that the RV144 vaccine protocol, which involved priming with a canarypox virus vector followed by boosting with recombinant gp120 protein, reduced HIV-1 infection by approximately 30% [1]. These results are encouraging, and indicate that poxviruses may be used as vectors for HIV-1 subunit vaccines.

However, the efficacy of the RV144 vaccine was only moderate, suggesting the need to improve either the vaccination regimen or the poxvirus vector used for delivery. One improvement that may elicit a more potent protective immune response is the use of a replication-competent vaccinia virus (VV) vector rather than the non-replicating canarypox vector.

We previously reported that a heterologous prime-boost vaccination protocol using a recombinant m8Δ (rm8Δ) virus (m8Δ-pSFJ-JRCSFenv), which expresses the HIV-1JR-CSF envelope glycoprotein, and a recombinant Sendai virus (rSeV), SeV-JRCSFenv, elicited both HIV-1 Env-specific humoral and cell-mediated immune responses [2]. This may be a promising vaccination protocol to protect against HIV-1 infection. The aim of the present study is to further optimize this regimen.

The replication-competent VV strain, LC16m8, is a smallpox vaccine licensed for use in Japan. It has been used in 100,000 people without any serious adverse effects [3]. LC16m8Δ (m8Δ) is a genetically stable derivative of LC16m8, which is safer than the parental LC16m8 virus but shows the same degree of antigenicity [4]. Moreover, immunization with m8Δ protects mice against infection with virulent VV much more efficiently than the non-replicating VV strain, MVA [4]. Thus, m8Δ may be a promising VV vector for use in vaccines against infectious diseases.

Three types of promoter (early, intermediate, and late) have been identified in VV. Antigens that are highly expressed under the control of a powerful late promoter are generally considered to be potent inducers of a strong immune response [5]. However, early promoters appear to elicit stronger cytotoxic T lymphocyte (CTL) responses [6,7]. In some cases, the propagation of VV *in vitro* is suppressed in the presence of high levels of foreign antigen. Therefore, the balance between antigen expression and viral propagation *in vivo* may be crucial for optimal immunogenicity.

* Corresponding author. Tel.: +81 11 706 7543; fax: +81 11 706 7543.
E-mail address: zhangxf@igm.hokudai.ac.jp (X. Zhang).
[1] Current address: Viral Infectious Diseases Unit, RIKEN, Hirosawa, Wako, Saitama 351-0198, Japan.

0264-410X/$ – see front matter © 2013 Elsevier Ltd. All rights reserved.
http://dx.doi.org/10.1016/j.vaccine.2013.12.022

The p7.5 promoter is an early–late promoter that was identified in 1984 and is widely used for the construction of live VV-vectored vaccines. Because the levels of gene expression driven by the p7.5 promoter have yet to be optimal, a more potent promoter, pSFJ1-10, was constructed, which enables the genes of interest to be expressed at higher levels during both the early and late phases of the infection cycle [8,9].

Here, we compared the immunogenicity and safety of two rm8Δs that express HIV-1 Env under the control of the p7.5 or pSFJ1-10 promoters. Both were tested in a vaccination protocol that involved priming with rm8Δ followed by boosting with rSeV. We found that one of the vectors preferably induced humoral responses against HIV-Env, whereas the other primarily induced cellular immune responses. These findings suggest that it may be possible to select vaccine vectors that induce favorable immune responses. In suckling mice, both rm8Δ-p7.5-JRCSFenv and rm8ΔpSFJ-JRCSFenv were relatively less virulent than LC16m8Δ. Our results may provide important information to develop HIV-1 vaccine for clinical trials.

2. Materials and methods

2.1. Cells and viruses

The RK13 cell line was cultured in RPMI1640 supplemented with 10% FCS at 37 °C in an atmosphere containing 5% CO_2. BHK, TZM-bl [10,11], 293T and L929 cell lines were cultured in DMEM supplemented with 10% FCS. VV LC16m8Δ, m8ΔVNC110 that harbors multiple cloning site in the HA gene of LC16m8Δ genome, m8Δ-pSFJ-JRCSFenv and SeV-JRCSFenv, which express gp160 of HIV-1 JRCSF, and canarypox virus were described previously [2].

2.2. Construction of the LC16m8Δ expressing JR-CSFenv under the control of the p7.5 promoter

To construct LC16m8Δ-p7.5-JRCSFenv, a transfer plasmid that harbors the HIV-1 JR-CSF env gene downstream of the p7.5 VV promoter was first constructed. The gp160-encoding region was amplified from pJWJRCSFenvΔEcoR1 (the template) by PCR using the following primer pair: JRCSFenv F1 (AGTGGATCCGCCACCATGAGAGTGAAGGGGATCAGGAAG; BamH1 site underlined) and JRCSFenvR1 (TTAGAGCTCTTATAGCAAAGCCCTTTCCAAGCC; Sac1 site underlined). The VV transcription termination signals (TTTTTNT) within the env gene sequence were synonymously mutated *in vitro* using a mutagenesis kit (Stratagene). The env fragment was then digested with Sac1 and ligated into the pVR1 vector [12], which had been digested with Sac1 and Sma1. BHK cells, which had been infected with canarypox virus, were then co-transfected with the resultant plasmid and LC16m8Δ genomic DNA to generate VV LC16m8Δ-p7.5-JRCSFenv. HA^- recombinants were selected using erythrocytes isolated from white leghorn chickens (Sankyo Labo Service Corporation, Inc.) [13,14]. Expression of HIV-1 Env protein was examined by Western blotting and plaque immunostaining.

2.3. Western blotting

Vaccinia-infected-RK13 cells were lyzed and the proteins separated in 10% SDS-PAGE gels. Immunoblot analysis was performed with human antiserum from a HIV-1-infected patient or monoclonal mouse anti-β actin antibody, followed by alkaline phosphatase-conjugated anti-human or mouse IgG (Promega). Proteins were visualized using NBT/BCIP (Sigma).

2.4. Plaque immunostaining

RK13 cells were cultured in 6-well plates and infected with recombinant VV (at approximately 100 plaque forming unit (pfu)/well). The cells were incubated with the virus for 72 h at 33 °C, fixed with 2% paraformaldehyde solution, and permeabilized by incubating with 0.5% Nonidet P-40 for 1 min. The fixed cells were blocked with 5% skimmed milk (in PBS) for 30 min at room temperature and incubated with the primary antibody (HIV-1 infected human serum; diluted 1000-fold) for 1 h at room temperature, followed by the secondary antibody (alkaline phosphatase-conjugated anti-human IgG (Promega); diluted 2500-fold). The plaques were then stained with NBT/BCIP.

2.5. Propagation potential of rm8Δ

To evaluate the propagation potential of LC16m8Δ and its recombinants, RK13, 293T and L929 cells (3×10^5) were infected with the viruses at a multiplicity of infection of 3 and then incubated for 24 h at 33 °C. Progeny viruses were harvested and titrated on a monolayer of RK13 cells in a plaque assay.

2.6. Immunization of mice

Seven-week-old female C57BL/6J mice (CLEA Japan) were administered with LC16m8Δ's recombinants (each at 1×10^7 pfu by skin scarification). Eight weeks later, the mice were boosted with rSeV expressing JRCSFenv (4×10^7 cell-infectious unit (CIU)) *via* intranasal administration (i.n.). Mice were sacrificed at 2 or 8 weeks after the final immunization, and serum and spleen samples were collected.

2.7. Intracellular cytokine staining (ICS) of splenocytes

Env-specific cellular immune responses were measured using an ICS assay as described previously [2]. The percentage of IFN-γ^+CD107a$^+$ T cells within the CD4- or CD8-gated lymphocyte populations were determined using a FACSCanto flow cytometer (BD biosciences) and the data were analyzed using FlowJo software (Tree Star).

2.8. Evaluation of neutralizing activity

The HIV-1 neutralizing activity of the mouse sera was measured in a TZM-bl cell-based assay as previously described [2,15,16].

2.9. Measurement of anti-Env antibody levels by ELISA

The titer and avidity of the anti-HIV-1 Env IgG antibodies in the mouse sera were determined by ELISA as described previously [2].

2.10. Safety of m8Δs

To evaluate the safety of the LC16m8Δ and m8Δ recombinants, 10 μl of a serially diluted solution that contains 10^3–10^7 pfu of rm8Δs was injected intracerebrally (i.c.) into 10 to 17 of 2–3-day-old suckling Crlj:CD1 (ICR) mice (Charles River) [17]. Survival was monitored daily for 2 weeks and the 50% lethal dose (LD50) was calculated as described in a figure legend.

2.11. Statistical analysis

Statistical analysis was performed using Student's *t*-test (Microsoft Excel version 11.6.6). *P* values of <0.05 were

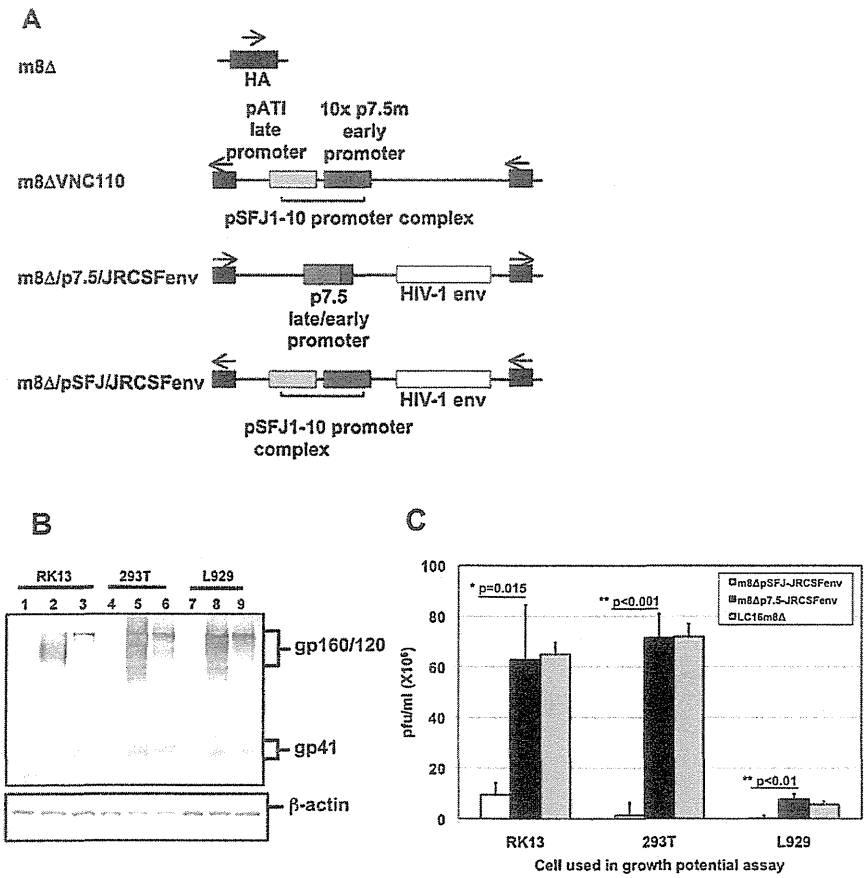

Fig. 1. Construction of the Env-expressing vaccinia vector, Env expression, and virus propagation. (A). Schematic illustration showing the structure of the hemagglutinin (HA) gene region within LC16m8Δ and its derivatives. Arrows indicate the direction of the HA coding frame. (B). Comparison of Env expression in cells infected with m8Δ-pSFJ-JRCSFenv or m8Δ-p7.5-JRCSFenv. One microgram of cell lysate derived from RK13 (rabbit kidney epithelial), 293T (human embryonal kidney cell line) and L929 (mouse fibroblastoid line) cells infected with rVV was subjected to SDS-PAGE and analyzed by Western blotting as described in Section 2. Lanes 1, 4, and 7 represent the cells infected with LC16m8Δ, lanes 2, 5, and 8, m8Δ-pSFJ-JRCSFenv; Lanes 3, 6, and 9, m8Δ-p7.5-JRCSFenv. (C) Comparison of the growth potential of the LC16m8Δ constructs. Viruses were recovered from RK13, 293T, and L929 cells 24 h after infection and titrated in a plaque assay. Data represent the mean ± SD ($n = 4$).

considered significant. The survival of virus-injected suckling mice was evaluated using the log-rank test (R version 2.15.1).

3. Results

3.1. In vitro properties of rm8Δ expressing JR-CSFenv under the control of different promoters

We previously constructed m8Δ-pSFJ-JRCSFenv, which expresses the HIV-1JR-CSF env gene under the control of the high expression pSFJ1-10 promoter, and showed that it elicited HIV-1 Env-specific cellular and humoral responses when used in combination with the Sendai vector, SeV-JRCSFenv [2]. However, because an rVV that moderately expresses a foreign gene, but propagates better, might elicit more potent immunological responses, we constructed recombinant m8Δ expressing JR-CSFenv under the control of the p7.5 promoter (which is a moderate driver of foreign gene expression) (Fig. 1A). We first compared expression of the Env protein in various cells infected with m8Δ-p7.5-JRCSFenv or m8Δ-pSFJ-JRCSFenv by Western blotting (Fig. 1B). Regardless of the cell type, m8Δ-p7.5-JRCSFenv produced several-fold less gp120/160 than m8Δ-pSFJ-JRCSFenv. In addition, the bands corresponding to gp120/160 expressed by cells infected with m8Δ-pSFJ-JRCSFenv were much broader than those expressed by cells infected with m8Δ-p7.5-JRCSFenv. Meanwhile, titration of the progeny virus after one-step growth revealed that the growth potential of rVVs in mouse L929 cells are 10 times lower than that in human 293T cells and rabbit RK13 cells (Fig. 1C). Nevertheless, m8Δ-p7.5-JRCSFenv showed growth potential similar to that of the parental m8Δ, and significantly higher (6–50-fold) than that of m8Δ-pSFJ-JRCSFenv (Fig. 1C). This indicates that overexpression of the foreign gene suppresses viral propagation.

3.2. Immunogenicity of m8Δ-p7.5-JRCSFenv and m8Δ-pSFJ-JRCSFenv

We next compared the immunogenicity of m8Δ-p7.5-JRCSFenv and m8Δ-pSFJ-JRCSFenv by using them to prime mice, which were then boosted with SeV-JRCSFenv according to the schedule outlined in Fig. 2A. Splenocytes were isolated, stimulated with a mixture of HIV-1 consensus subtype B Env (15-mer) peptides (NIH AIDS reagent program, No. 202/203; corresponding to aa 805–819 and aa 809–823 of gp160), the two most immunogenic HIV-derived peptides, and then examined by ICS [2]. The percentage of HIV-1 Env-specific IFN-γ-secreting $CD107a^+CD8^+$ T cells was then calculated. A representative gating strategy is shown in Fig. 2B. Vaccination with m8Δ-pSFJ-JRCSFenv and m8Δ-p7.5-JRCSFenv elicited HIV-1JR-CSF Env-specific CTL responses. Mice primed with m8Δ-p7.5-JRCSFenv showed higher levels of HIV-1 Env-specific IFN $\gamma^+CD107a^+CD8^+$ T cells than mice primed with m8Δ-pSFJ-JRCSFenv (Fig. 2C; 12.8 ± 1.2% *vs.* 7.8 ± 2.1%; $p = 0.002$). The proportion of IFN $\gamma^+CD107a^+CD8^+$ T cells in both groups somewhat

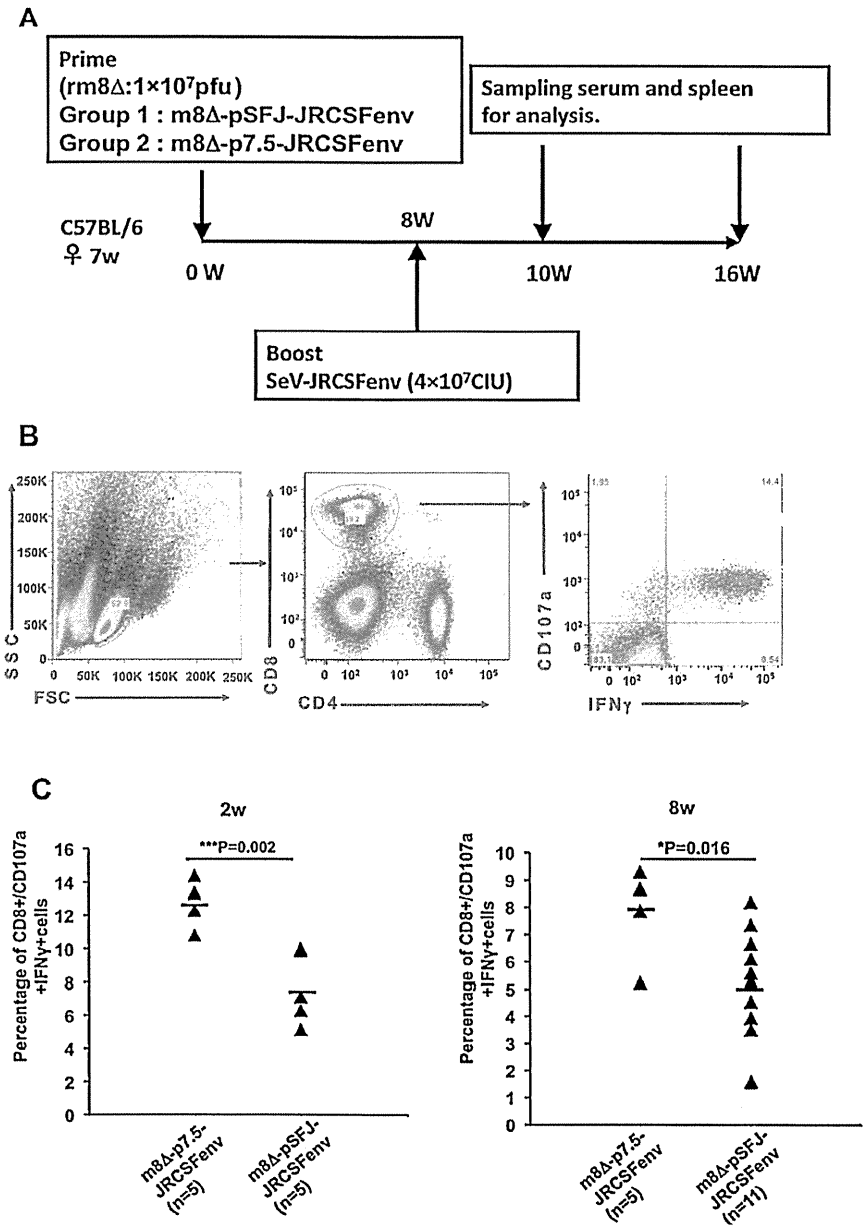

Fig. 2. The p7.5 promoter induces more efficient production of Env-specific CTL responses than the pSFJ promoter. (A) Schematic illustration showing the rm8Δ prime/rSeV boost vaccination protocol. Seven-week-old female C57BL/6J mice were vaccinated with LC16m8Δ's recombinants (16 mice for m8Δ-pSFJ-JRCSFenv (group 1) and 10 mice for m8Δ-p7.5-JRCSFenv (group 2); each at 1×10^7 pfu) followed by a boost with SeV-JRCSFenv (4×10^7 CIU). Blood samples and spleen tissues were examined at the indicated time points. (B) Representative diagram showing FACS analysis of HIV-1 Env-specific IFN-γ-secreting CD107a⁺CD8⁺ T cells derived from vaccinated mouse splenocytes. (C) Comparison of Env-specific cellular immune response between the two vaccinated groups at 2 and 8 weeks post-SeV boost.

declined at 8 weeks post-boost; however, the difference between the groups was maintained ($p = 0.016$). We next measured the levels of Env-specific Abs (Fig. 3A) and anti-HIV-1-neutralizing Abs (Fig. 3B) in mice sera. The levels of anti-HIV-1 Env-specific IgG were 6–7-fold higher in mice immunized with m8Δ-pSFJ-JRCSFenv than in mice immunized with m8Δ-p7.5-JRCSFenv; this was in sharp contrast to the observed cellular responses (Fig. 2). The difference of humoral immunity had already been detected 6 weeks after rm8Δ prime (supplementary data). The uneven of sample numbers between two groups did not introduce bias into the data, since we obtained the same result when two groups have the same number of animals (data not shown). Sera from both groups of mice showed neutralizing activity against a tier 1 pseudotyped HIV-1 strain, SF162, but only after rSeV boost, and no neutralization activity against tier 2 HIV-1 had been detected. At both 2 and 8 weeks post-SeV-JRCSFenv boost, the neutralizing competency of sera from mice immunized with m8Δ-pSFJ-JRCSFenv was marginally stronger than that of mice immunized with m8Δ-p7.5-JRCSFenv; however, the difference was not significant (Fig. 3B). We also measured the avidity of the anti-Env Abs in both groups: no significant difference was observed (Fig. 3C). Since the m8Δ-pSFJ-JRCSFenv prime/SeV-JRCSFenv boost elicited greater HIV-1 Env-specific antibody responses, we next asked whether this antibody titer is maintained over the long-term. We followed a subgroup of mice

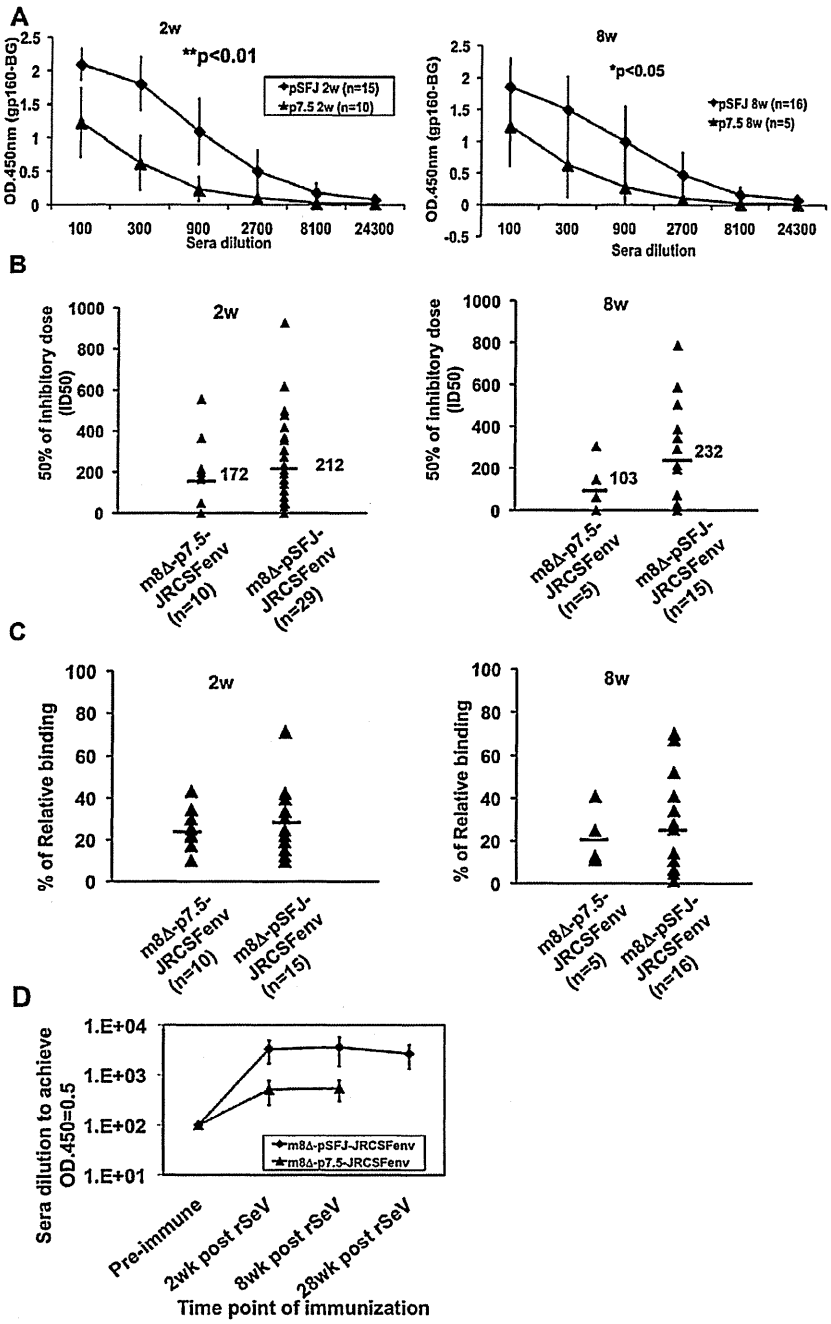

Fig. 3. m8Δ-pSFJ-JRCSFenv induces stronger humoral immune responses than m8Δ-p7.5-JRCSFenv (A). Comparison of Env-specific antibody levels. Serum from individual immunized mice was analyzed in a HIV-1JR-CSF gp160 ELISA as described previously (Ref. [2]). The plates were developed with an HRP-conjugated anti-mouse IgG antibody. The Env-specific antibody titer was determined by subtracting the background values at OD450. Data represent the mean ± SD of the Env-specific antibody titer of all animals in each group. Env binding antibody titers measured at 2 and 8 weeks post-rSeV boost are shown. (B) Comparison of anti-HIV-1 neutralizing antibody activity in sera from the two groups of immunized mice. We included more previously accumulated mice samples that subjected to the same immunization procedure as group 1 in Fig. 2. The 50% inhibitory dose (ID50) against an HIV-1 SF162 env-pseudotyped virus was measured using TZM-bl cells (a CD4- and CCR5-expressing derivative of HeLa cells). The neutralizing activity of mouse sera is shown at 2 and 8 weeks post-SeV boost. (C) Comparison of the avidity of HIV-1 Env-specific anti-sera from the two groups at 2 and 8 weeks post-SeV boost as described previously (Ref. [2]). (D) Comparison of HIV-1 Env-specific antibody induction dynamics between the two groups after the rSeV boost.

treated with this vaccination regimen for 28 weeks after the Sendai virus boost and found that the anti-HIV-1 Env antibody titer was maintained throughout the observation period (Fig. 3D).

3.3. *Safety evaluation of the rm8Δ in suckling mice*

To evaluate the safety of rm8Δ, we i.c.-injected suckling mice with m8Δ, m8ΔVNC110, m8Δ-pSFJ-JRCSFenv, or m8Δ-p7.5-JRCSFenv. At 2 weeks post-injection, more of the mice in the m8ΔVNC110- and m8Δ-pSFJ-JRCSFenv-injected (at 10^4 and 10^5 pfu) groups survived compared with those in the m8Δ-p7.5-JRCSFenv-injected group (Fig. 4B–D). LC16m8Δ, which should be safe for human use, showed the highest mortality (Fig. 4A). The median lethal doses (LD50) for each strain were as follows: LC16m8Δ, $<10^3$ pfu; m8Δ-p7.5-JRCSFenv, 5.5×10^3 pfu; m8Δ-pSFJ-JRCSFenv, 1.4×10^5 pfu; and m8ΔVNC110, 5.75×10^5 pfu

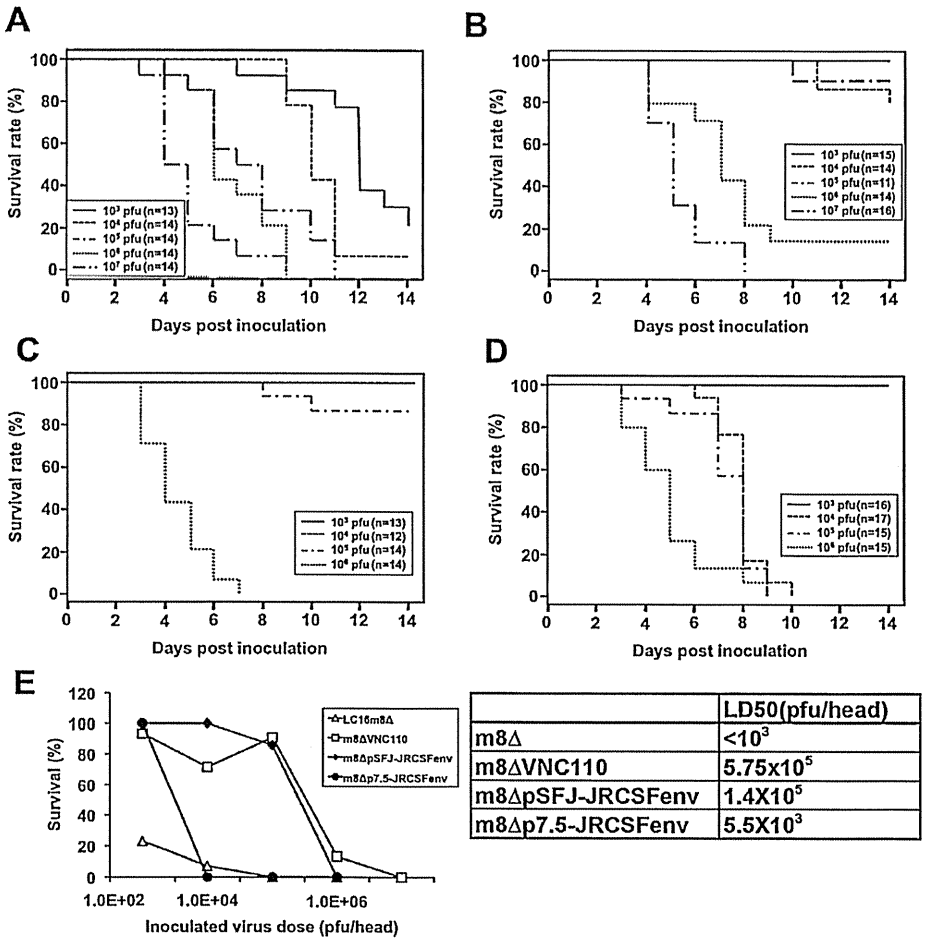

	LD50(pfu/head)
m8Δ	$<10^3$
m8ΔVNC110	$5.75x10^5$
m8ΔpSFJ-JRCSFenv	$1.4X10^5$
m8Δp7.5-JRCSFenv	$5.5X10^3$

Fig. 4. m8Δ-pSFJ-JRCSFenv is safer than m8Δ-p7.5-JRCSFenv *in vivo*. Cumulative survival curves for vaccinated suckling mice are shown. Mice were injected with LC16m8Δ (A), m8ΔVNC110 (B), m8Δ-pSFJ-JRCSFenv (C), or m8Δ-p7.5-JRCSFenv (D). Percentage of survival at 2 weeks post inoculation was plotted to make a survive curve using Microsoft Excel (version 11.6.6) and the 50% lethal dose (LD50) was calculated according to the Trendline of the curve. The LD50 for each VV is shown (E). The numbers of the mice used for each dose are indicated in the chart. Statistical analysis was performed using the log-rank test.

(Fig. 4E). These results suggest that both m8Δ-p7.5-JRCSFenv and m8Δ-pSFJ-JRCSFenv may be safer for use in humans.

4. Discussion

An effective HIV-1 vaccine should induce long-lasting humoral and cellular immunity against HIV-1. A replication-competent VV would be a good candidate for such a vaccine because recombinant VV can induce both antigen-specific CTL and antibody responses. In addition, the process of viral replication may allow the repeated presentation of viral antigens, leading to affinity maturation of both antibodies and T cell receptors. LC16m8Δ-JRCSFenv is a replication-competent vaccinia vector that induces HIV-1 Env-specific cellular and humoral immune responses when used in combination with a Sendai virus vector [2]. Here, we tried to optimize this vaccination regimen by using HIV-1 Env recombinant VV vectors expressed under the control of different promoters. We found that viruses expressed under the control of these different promoters induced different cellular and humoral immune responses. m8Δ-pSFJ-JRCSFenv induced increased production of anti-HIV-1 Env-specific Abs when compared with m8Δ-p7.5-JRCSFenv. By contrast, m8Δ-p7.5-JRCSFenv induced the production of more HIV-1 Env-specific IFN-γ-secreting $CD107a^+CD8^+$ T cells. These results suggest that the induction of Env-specific CTL and humoral responses may be dependent upon different presentation pathways and/or different structures of the Env protein. The peptides used to stimulate the splenocytes in the ICS assay correspond to the 3′ domain of gp41, since previous mapping of the consensus subtype B Env peptide pool identified peptides comprising aa 805–819 and aa 809–823 as the best immunogens [2]. It also indicated that gp41 but not gp120 is a more potent inducer of cellular immunity when liberated from gp160 than it is when buried in gp160. The amount of gp41 in m8Δ-p7.5-JRCSFenv-infected 293T and L929 cells are comparable with that infected with m8Δ-pSFJ-JRCSFenv and even more in m8Δ-p7.5-JRCSFenv-infected RK13 cells, which is different from the case of gp160/gp120 (Fig. 1B). Considering the better replication of m8Δ-p7.5-JRCSFenv (Fig. 1C), we may expect that repetitive antigenic stimulation, which favors CTL induction, strengthens the immunogenicity of gp41 that is derived from m8Δ-p7.5-JRCSFenv to induce production of Env-specific IFN-$\gamma^+CD107a^+CD8^+$ T cells. The relatively lower ratio of gp41 to gp160/gp120 in m8Δ-pSFJ-JRCSFenv-infected cells than m8Δ-p7.5-JRCSFenv cells indicates that the cleavage of gp160 to gp120 and gp41 was less efficient due to overexpression of Env.

On the other hand, the efficient production of anti-Env-specific antibodies may require higher expression of HIV-1 Env in primarily infected cells. The 6–7-fold higher level of the HIV-1 Env binding antibody titer observed in mice immunized with m8Δ-pSFJ-JRCSFenv is consistent with the higher levels of Env observed